
Electronic Thesis and Dissertation Repository

4-18-2017 12:00 AM

Characterizing Ferroportin Trafficking in Macrophages During Phagocytosis

Taylor J. Farrell
The University of Western Ontario

Supervisor
Dr. David E Heinrichs
The University of Western Ontario

Graduate Program in Microbiology and Immunology
A thesis submitted in partial fulfillment of the requirements for the degree in Master of Science
© Taylor J. Farrell 2017

Follow this and additional works at: <https://ir.lib.uwo.ca/etd>



Part of the [Cell Biology Commons](#), and the [Immunity Commons](#)

Recommended Citation

Farrell, Taylor J., "Characterizing Ferroportin Trafficking in Macrophages During Phagocytosis" (2017).
Electronic Thesis and Dissertation Repository. 4482.
<https://ir.lib.uwo.ca/etd/4482>

This Dissertation/Thesis is brought to you for free and open access by Scholarship@Western. It has been accepted for inclusion in Electronic Thesis and Dissertation Repository by an authorized administrator of Scholarship@Western. For more information, please contact wlsadmin@uwo.ca.

ABSTRACT

Macrophages are important mediators of innate immunity and nutritional immunity via modulation of essential nutrients like iron during bacterial infection. Ferroportin (Fpn), an iron-exporting protein, is found on the plasma membrane of macrophages and, if not modulated during phagocytosis, would transport iron into phagosomes and supply phagocytosed bacteria with iron. Interestingly, the fate of Fpn during phagocytosis and bacterial infection remains unknown. I generated a Fpn-GFP fusion protein and, using fluorescence microscopy, demonstrated that, during phagocytosis in RAW264.7 macrophages, Fpn is removed from phagosomes containing IgG-coated beads or *Staphylococcus aureus*. Further, Fpn is present on Rab5-containing phagosomes but absent from PI(3)P- and LAMP1-positive phagosomes indicating Fpn removal occurs early during phagosome maturation. Co-localization analysis revealed that markers of cellular recycling pathways, Rab4 and transferrin receptor, do not co-localize with Fpn. Thus, my data support the conclusion that macrophages restrict Fpn residence on phagosomes presumably to prevent iron transport into phagosomes.

Keywords: iron, ferroportin, trafficking, macrophages, phagocytosis, nutritional immunity

ACKNOWLEDGEMENTS

First and foremost, I would like to thank my supervisor, Dr. David Heinrichs, for his instrumental insight into my project and the scientific learning process in general. He was always willing to discuss my research and writing whenever I had questions. I'd also like to thank him for providing helpful guidance in experimental design, for helping to steer my project in the right direction, and for demanding high quality work in all my endeavors. Also, I'd like to extend my thanks for his encouragement in attending multiple conferences during which I learned valuable skills as a scientific researcher.

I would also like extend a special thank you to Dr. Ron Flannagan for countless discussions and invaluable suggestions, for lessons and aid in fluorescence microscopy, and for reading this thesis. He helped me realize science is also an art as he is excellent at thinking outside the box and devising creative solutions to difficult questions.

I offer my sincerest gratitude to my advisory committee members Dr. Jimmy Dikeakos and Dr. Sung Kim for helpful recommendations and critical insight throughout my project. Also thank you to both for reading my thesis and providing helpful feedback.

I would also like to thank all other members of the Heinrichs lab for the entertaining discussions and endless support over the course of my time as a graduate student. A special thanks to Holly Laakso and Julie Kaiser, for without you, who would have listened to the interesting (if random) information I've learned from listening to podcasts while on the microscope. Also, I'd like to thank members of the Stuff You Should Know podcast for keeping me sane during the hours on the microscope.

Lastly, thank you to all my friends and family for their unyielding support throughout these two years in graduate school. This accomplishment would not have been possible without them.

TABLE OF CONTENTS

ABSTRACT.....	ii
ACKNOWLEDGEMENTS.....	iii
TABLE OF CONTENTS.....	iv
LIST OF TABLES.....	vii
LIST OF FIGURES.....	viii
LIST OF ABBREVIATIONS.....	ix
CHAPTER 1 – LITERATURE REVIEW.....	1
1.1 Introduction to innate immunity.....	1
1.2 Iron.....	2
1.2.1 Host iron binding proteins.....	2
1.2.2 Iron toxicity.....	3
1.2.3 Host cellular iron homeostasis.....	4
1.2.4 Systemic iron homeostasis and the macrophage.....	4
1.2.5 Iron-related diseases.....	5
1.2.6 Bacterial iron acquisition.....	6
1.3 Nutritional Immunity.....	8
1.3.1 Iron restriction in the host.....	8
1.3.2 NRAMP1.....	9
1.3.3 DMT1.....	10
1.3.4 Inflammatory hypoferremia.....	10
1.3.5 Manganese and zinc binding proteins.....	11
1.3.6 Copper transporting proteins.....	12
1.4 Ferroportin.....	13
1.4.1 Function and structure.....	13
1.4.2 Mechanism of iron binding and transport.....	13
1.4.3 Ferroportin regulation.....	14
1.4.4 Ferroportin-related diseases.....	15

1.4.5 Ferroportin and infection	15
1.5 Phagocytes	16
1.5.1 Macrophages	16
1.5.2 Phagocytosis and phagocytic receptors	17
1.5.3 Phagosome maturation.....	18
1.5.4 Antimicrobial effectors of macrophages.....	20
1.5.5 Bacteria that manipulate phagocytosis.....	20
1.6 Endocytosis and endocytic protein trafficking	21
1.6.1 Rab GTPases	22
1.6.2 Recycling	22
1.6.3 Degradation.....	22
1.7 Project rationale and hypothesis	23
CHAPTER 2 – MATERIALS and METHODS	26
2.1 Reagents.....	26
2.2 Bacterial strains, plasmids and culture conditions.....	26
2.3 Mammalian cell culture and transfection.....	30
2.4 Silica bead opsonization and phagocytosis.....	30
2.5 Immunofluorescence staining of LAMP1.....	30
2.6 Concanamycin A treatment and LysoTracker® loading of macrophages	31
2.7 Wide-field fluorescence microscopy	31
2.8 Confocal microscopy	32
2.9 Deconvolution and image analysis	32
2.10 Statistical analysis.....	33
CHAPTER 3 – RESULTS	34
3.1 Fpn is removed from phagosomes harbouring <i>S. aureus</i> or IgG-coated beads	34
3.2 Selective exclusion of Fpn from LAMP1-positive phagosomes	38
3.3 Inhibition of acidification does not prevent Fpn removal from the phagosome.....	40
3.4 Fpn and TfnR do not co-localize in the cytoplasm of macrophages.....	42
3.5 TfnR co-localizes with Rab4 while Fpn does not.....	44
3.6 Early PI(3)P-positive phagosomes show more Fpn depletion than TfnR depletion.....	46

3.7 The PI3K inhibitor LY294002 alters cellular distribution of TfnR but not Fpn	48
3.8 PI3K-independent removal of Fpn from the phagosome.....	50
3.9 Fpn co-localizes with Rab5 during the early stages of phagosome maturation.....	52
3.10 Fpn removal is temporarily delayed in cells expressing constitutively active Rab5	54
3.11 Fpn is present on some Rab7-containing phagosomes	57
CHAPTER 4 – DISCUSSION and FUTURE DIRECTIONS.....	59
REFERENCES	66
APPENDIX 1	81
CURRICULUM VITAE.....	83

LIST OF TABLES

Table		Page
Table 1.	Bacterial strains and plasmids used in this study	27
Table 2.	Oligonucleotides used for cloning	29

LIST OF FIGURES

Figure		Page
Figure 1.	Phagosome maturation	19
Figure 2.	Postulated mechanisms of Fpn removal from the phagosome	25
Figure 3.	Fpn is depleted from the phagosome as it matures	36
Figure 4.	Selective exclusion of Fpn from LAMP1-positive phagosomes	39
Figure 5.	Phagosomal loss of Fpn is not altered upon inhibition of acidification	41
Figure 6.	Fpn and TfnR do not co-localize in the cytoplasm of macrophages	43
Figure 7.	TfnR co-localizes with Rab4 while Fpn does not	45
Figure 8.	Early PI(3)P-positive phagosomes show more Fpn depletion than TfnR depletion	47
Figure 9.	PI3K inhibitor LY294002 alters the distribution of TfnR but not Fpn throughout the cell	49
Figure 10.	PI3K-independent removal of Fpn from the phagosome	51
Figure 11.	Fpn co-localizes with Rab5 during the early stages of phagosome maturation	53
Figure 12.	Fpn removal is temporarily delayed in cells expressing constitutively active Rab5	55
Figure 13.	Fpn is present on some Rab7-containing phagosomes	58
Figure S1.	Fpn-GFP localizes to the plasma membrane and does not perturb phagocytosis in RAW264.7 macrophages	82

LIST OF ABBREVIATIONS

ATP	Adenosine triphosphate
CA	Constitutively active
CcA	Concanamycin A
CFUs	Colony forming units
CP	Calprotectin
DMSO	Dimethyl sulfoxide
DNA	Deoxyribonucleic acid
DMT1	Divalent metal transporter 1
EGF	Epidermal growth factor
EGFR	Epidermal growth factor receptor
ERC	Endocytic recycling compartment
Ery	Erythromycin
ESCRT	Endosomal sorting complex required for transport
FBS	Fetal bovine serum
Fpn	Ferroportin
Fur	Ferric uptake regulator
GAPs	GTPase activating proteins
GDP	Guanosine diphosphate
GEFs	Guanine nucleotide exchange factors
GFP	Green fluorescent protein
GM-CSF	Granulocyte-macrophage colony-stimulating factor
GTP	Guanosine triphosphate
HCP1	Heme carrier protein 1
HH	Hereditary hemochromatosis
Hr	Hour
IFN	Interferon
IgG	Immunoglobulin G
IL	Interleukin
ILV	Intraluminal vesicle

IRE	Iron responsive element
IRP	Iron responsive protein
Isd	Iron-regulated surface determinant
ITAM	Immunoreceptor tyrosine-based activation motif
Kan	Kanamycin
LAMP1	Lysosome-associated membrane protein-1
LPS	Lipopolysaccharide
M-CSF	Macrophage colony-stimulating factor
MFS	Major facilitator superfamily
MVB	Multivesicular body
NADPH	Nicotinamide adenine dinucleotide phosphate
NETs	Neutrophil extracellular traps
NGAL	Neutrophil gelatinase-associated lipocalin
NO	Nitric oxide
NRAMP1	Natural resistance-associated macrophage protein 1
PAMPs	Pathogen associated molecular patterns
PBS	Phosphate buffered saline
PCBP2	Poly(rC)-binding protein 2
PCR	Polymerase chain reaction
PFA	Paraformaldehyde
PI	Phosphatidylinositol
PI3K	Phosphatidylinositol-3-kinase
PI(3)P	Phosphatidylinositol-3-phosphate
PI(4)P	Phosphatidylinositol-4-phosphate
PI(3,4,5)P ₃	Phosphatidylinositol-3,4,5-trisphosphate
RAW	RAW264.7 macrophages
RFP	Red fluorescent protein
ROI	Region of interest
RPMI	Roswell Park Memorial Institute
SD	Standard deviation
SEM	Standard error of the mean

SF	Serum free
Tfn	Transferrin
TfnR	Transferrin receptor
TSB	Tryptic Soy broth
vATPase	Vacuolar-ATPase
veh	Vehicle control
WT	Wild type

CHAPTER 1 – LITERATURE REVIEW

1.1 Introduction to innate immunity

Innate immunity is the first line of defense against invading pathogens and provides an immediate yet relatively short-lived defense against infection. Components of innate immunity include anatomical barriers, the microbiome, complement, nutrient restriction, and phagocytes, as have been previously reviewed (1–5). Infection occurs following a breach in the gastrointestinal, urogenital, respiratory tract, or the skin epithelium. The host attempts to prevent infection in multiple ways. For example: to prevent bacterial attachment, mechanical forces, such as the movement of cilia and air flow in the respiratory tract or the clearance of urine in the urogenital tract, are employed. Further, chemical cues such as antimicrobial peptides on the skin and acidic pH in the gastrointestinal tract limit bacterial growth. Colonization with commensal bacteria provides an additional barrier to invading microbes by competing with invading microbes for attachment sites and nutrients in a process termed colonization resistance (2, 6).

Augmentation of anatomical barrier function is provided by the humoral aspect of innate immunity which involves for example, the deposition of complement on invading microbes (3). Complement proteins are found in the circulation in inactive forms and recognize pathogens using highly conserved pathogen-associated molecular patterns (PAMPs). When recognized, the complement protein C3 is deposited onto the microbial surface and activated, thereby targeting the microbe for lysis or ingestion by phagocytes. While crucial to innate immunity, complement was originally named due to the functional complementation it provides phagocytes – a component of innate immunity important to this project. Phagocytes are absolutely essential to the immune system as their bactericidal function is a crucial part of the innate immune system and also provides a link to adaptive immunity by initiating its activation (5).

The final component of innate immunity is nutrient restriction. Nutrient restriction includes the purposeful withholding of essential nutrients, such as iron and manganese, by the host to limit pathogen growth. The many mechanisms of nutrient withholding during bacterial infection are collectively referred to as nutritional immunity (4, 7). Important to this project is the intersection between phagocytes and nutritional immunity,

specifically concerning iron, and these components are reviewed in more detail below.

1.2 Iron

Iron is one of the most abundant elements on Earth (8) and is an essential nutrient for nearly all life forms – one of the only known exceptions being the microorganism *Borrelia burgdorferi* (9). Iron plays a key role in many cellular processes for both the host and pathogenic microbes. Many iron-requiring processes are essential for survival and include oxygen transport, cellular respiration, cell cycle control, and DNA replication and repair (10, 11). The ability of iron to act in such diverse processes is due to the redox potential it provides by alternating between ferrous (Fe^{2+}) and ferric (Fe^{3+}) states, with a redox that spans approximately 1 volt. While bacterial iron homeostasis and acquisition are briefly reviewed in a later section (section 1.2.6), for the purposes of this study, the focus is on the roles of iron and iron-binding proteins in host processes.

1.2.1 Host iron binding proteins

Generally, iron is found throughout the body in one of two forms: heme-iron or non-heme iron. Heme-iron is one of the most physiologically important forms of iron and is also the most abundant, making up approximately 60% of total iron in the human body. Structurally, heme consists of a planar porphyrin ring which allows for the coordination of one ferrous iron atom via four nitrogen atoms (12) and is incorporated into many enzymes as a cofactor (13, 14). The heme-iron complex is utilized in many processes, the most notable being oxygen transport. Erythrocytes contain high levels of hemoglobin, a heme binding protein. Binding to heme allows hemoglobin to bind to oxygen and facilitate delivery of oxygen from the lungs throughout the tissues. Other heme utilizing proteins include myoglobin, which acts similarly to hemoglobin but in muscle tissue, and cytochrome c oxidase, a molecule found in both bacterial and eukaryotic electron transport chains that aids in establishing a proton gradient for ATP synthesis.

Some proteins utilize iron in forms such as iron-sulfur clusters. Iron-sulfur clusters are protein co-factors that co-ordinate iron using cysteine residues (15). The electron transport flavoprotein ubiquinone-oxidoreductase is a component of the

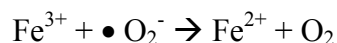
mitochondrial respiratory chain that utilizes iron-sulfur clusters to mediate transfer of electrons into the ubiquinone electron pool (16).

Other major sources of non-heme iron include ferritin and transferrin. Ferritin is the primary intracellular iron storage protein for both bacteria and eukaryotes (17). It is a globular protein composed of 24 subunits that forms a nanocage capable of internalizing and oxidizing ferrous iron and storing ferric iron. Iron storage by ferritin is important not only to prevent loss of iron but also to prevent formation of hydroxyl radicals (discussed in 1.2.2). Further, in iron deficient conditions, ferritin is degraded in lysosomes to yield an iron source (18). Transferrin (Tfn) is a glycoprotein found in the blood that can bind two atoms of ferric iron with high affinity (19, 20). Like ferritin, Tfn is important for maintaining iron in the non-toxic ferric form but also in facilitating cellular iron uptake and transporting iron from sites of absorption throughout the body.

1.2.2 Iron toxicity

Despite its importance to cellular function, cellular levels of free iron are strictly maintained to prevent cellular toxicity. This toxicity is due to the iron-dependent Haber-Weiss reaction that produces reactive oxygen species. The Haber-Weiss reaction consists of two parts, one of which utilizes Fenton chemistry: the reaction of ferrous iron (Fe^{2+}) and hydrogen peroxide (a by-product of aerobic respiration) to generate hydroxyl radicals, as shown in Equation 2 (21, 22).

Equation 1.



Equation 2. Fenton Reaction.



Net



Reactive oxygen species, including hydroxyl radicals, are powerful oxidizing agents that damage various biological molecules including lipids, proteins, and nucleic acids (23–25). This eventually leads to loss of molecular function and, ultimately, cellular death (26). For this reason, the host utilizes many mechanisms to rigorously limit cellular levels of free iron.

1.2.3 Host cellular iron homeostasis

Because of both its potential toxicity and its importance for cellular function, the host has evolved sophisticated mechanisms to strictly regulate iron absorption, transport, storage and utilization at the cellular level. The average human body contains between 3-5 g of iron which is obtained exclusively from dietary sources. Non-heme iron and heme-iron are absorbed into cells of the intestine using the importing proteins divalent metal transporter 1 (DMT1) (27, 28) and heme carrier protein 1 (HCP1) (29), respectively. DMT1 and HCP1 are membrane proteins expressed in the apical surface of epithelial cells in intestinal villi. Heme uptake is mediated by HCP1 (30, 31) and, while intracellular trafficking mechanisms of heme are poorly understood, once inside the cell heme is degraded via heme oxygenase thereby releasing iron which is then bound by the iron chaperone protein PCBP2 (poly(rC)-binding protein 2) (32, 33). Conversely, DMT1 binds to free iron and transports it into the cell which is then bound by PCBP2. PCBP2 shuttles imported iron to the storage protein ferritin or to the iron exporting protein called ferroportin (Fpn). Fpn is located at the basolateral membrane of intestinal epithelial cells where it exports iron out of the cell and into the blood (34–36). Interestingly, there is no known regulated, physiological means of excreting iron for the purposeful loss from the body. The only loss, apart from bleeding, is minimal and occurs via the sloughing of cells from epithelial surfaces like the skin and the gastroenteric/genitourinary tracts.

Due to the absence of a controlled excretion mechanism, the levels of cellular iron are strictly maintained by controlling absorption in the intestines and transport into circulation. During iron-limited conditions the expression of DMT1 increases in the duodenum to allow for increased absorption (37). Further, iron stored intracellularly in ferritin can be accessed by enhancing proteolytic degradation of ferritin (18). Alternatively, in iron-replete conditions, levels of Fpn expression at the membrane are decreased to prevent iron export into the circulation (38). This event is mediated by the peptide hepcidin which is the master regulator of systemic iron homeostasis (39).

1.2.4 Systemic iron homeostasis and the macrophage

In addition to maintaining cellular levels of iron, it is also imperative to regulate iron levels systemically. A key mediator of this process is the macrophage as they are

responsible for iron recycling via erythrophagocytosis (40). Erythrocytes represent the largest pool of iron within the human body due to the large amounts of hemoglobin contained within these cells (41). The large volume of hemoglobin enables erythrocytes to circulate throughout the body and deliver oxygen to tissues for up to 120 days at which point erythrocytes are recycled.

Macrophages, particularly in the spleen and liver, recognize senescent erythrocytes, internalize them via phagocytosis and then proteolytically degrade the internalized cell. Degradation allows the macrophage to extract iron from the cell and shuttle iron into different pathways. Iron may be exported out of the macrophage and into the circulation via Fpn, which is also expressed on the plasma membrane of macrophages (42). Once in circulation, iron is bound by Tfn and transported between sites of utilization and storage, mainly in hepatocytes and liver macrophages. Most of the recycled iron is supplied to erythrocyte precursor cells in the bone marrow.

In addition to iron recycling via erythrophagocytosis, macrophages also play a role in systemic iron regulation via interaction with hepcidin (43). Hepcidin is a 25-amino acid peptide hormone produced by the liver and is the primary regulator of iron absorption and distribution throughout the tissues (44). Iron excess stimulates production of hepcidin which then results in the internalization of Fpn (38). This decreases iron transport from macrophages into the circulation. Alternatively, iron deficiency inhibits hepcidin production which allows the release of iron stored within macrophages.

Macrophages play another important role in iron homeostasis in that they aid in generating hypoferremia during bacterial infection. This aspect of iron homeostasis is discussed further in later sections of this review (section 1.3.4). Nevertheless, maintenance of iron homeostasis is a complex process involving many factors at both cellular and systemic levels, many of which are mediated functionally by macrophages. Accordingly, disturbances in homeostasis can have potentially serious consequences.

1.2.5 Iron-related diseases

Iron is essential for cellular function and, as such, when iron homeostasis is disrupted serious disease can result. Iron-related diseases generally fit into one of two categories: iron overload or iron deficiency. Iron deficiency, one of the most common nutrient

deficiencies in the world, is generally caused by inadequate dietary intake (45). It can also be caused by an alteration in iron absorption due to the presence of certain substances such as the antibiotic fluoroquinolone. Fluoroquinolone is an iron chelator and therefore its presence in the intestine can result in reduced iron absorption (46). Chronic iron-deficiency can lead to anemia which is a decrease in red blood cells or hemoglobin in the blood.

Conversely, iron-overload diseases are often hereditary but can also be caused by repeated blood transfusions (47). One branch of inherited iron-overload disease is hereditary hemochromatosis (HH). There are four types of HH and they are categorized as follows: types 1 through 4 caused by mutations in genes HFE (encoding the human hemochromatosis protein) (48), HAMP (encoding hepcidin) (49), TFR2 (encoding transferrin receptor 2) (50), or SLC40A1 (encoding Fpn) (51, 52), respectively. HH type 4, sometimes referred to as Fpn disease, is discussed in more detail in section 1.4.4. Pathologically, iron-overload can cause cellular structural damage from physical accumulation of iron within the cell and oxidative damage due to the iron-mediated production of reactive oxygen species (25).

Interestingly, iron-overload diseases also have implications in susceptibility to infection. Patients with HH are more susceptible to infection by many different pathogens including by *Vibrio vulnificus* (53), *Yersinia enterocolitica* (54), and *Listeria monocytogenes* (55). Further, patients with iron-overload due to repeated blood transfusions also experience increased susceptibility to infection as well as increased severity of infection (56, 57) highlighting both the importance of iron homeostasis in the host but also, as mentioned above, the importance of iron to bacteria.

1.2.6 Bacterial iron acquisition

Iron is essential to many biological processes in bacteria including cellular respiration, electron transport, and DNA replication and repair. Environmental concentrations of free iron are relatively low since, at neutral pH in the presence of oxygen, iron precipitates. Moreover, in the context of infection, the host has evolved many mechanisms of iron-withholding to further reduce environmental concentrations of iron (discussed in depth in section 1.3). Like the host, iron concentrations within bacterial cells must be strictly

regulated since high concentrations can be toxic (discussed in section 1.2.3). As such, bacteria have evolved sophisticated iron-acquisition strategies that allow them to regulate iron import and overcome iron-limitation within the host (58).

Pathogens utilize transcriptional regulators to sense environmental iron and regulate gene expression accordingly. Gram-negative and some Gram-positive bacteria, such as *Staphylococcus* spp., utilize the ferric uptake regulator (Fur), an iron-sensing mechanism conserved across many bacterial species (59). Several mechanisms exist in bacteria for iron sensing, however, by far the most studied mechanism is through the activity of Fur. In iron-replete conditions, Fur is bound to ferrous iron as its corepressor. Iron-binding induces a conformational change in Fur allowing it to bind DNA and prevent target gene expression. In iron-limited conditions, Fur is not bound to iron and therefore does not bind DNA and repress gene expression. Many of the genes regulated by Fur relate specifically to iron acquisition, but some also relate to virulence, biofilm formation and the expression of anti-oxidative stress proteins (60).

Bacterial iron acquisition falls into generally one of three categories: heme-iron acquisition, siderophore-mediated iron acquisition, and free iron uptake. Heme-iron acquisition involves the extraction of heme or heme-binding proteins from sources within the host, transport of heme into the bacterial cell and eventual degradation of the heme moiety to release iron for bacterial use. A major heme acquisition mechanism in *S. aureus* and other Gram-positive pathogens is the Isd (iron-regulated surface determinant) system (61). Further, several bacterial pathogens use secreted heme-binding proteins, called hemophores, to bind heme and deliver it back to the bacterial surface for eventual transport. Another major iron-acquisition strategy of bacteria involves siderophores. Siderophores are secreted, low-molecular weight, high affinity iron chelators. In response to iron deprivation, bacteria secrete siderophores to scavenge residual free iron in the environment and to appropriate Tfn- and lactoferrin-bound iron. The last iron acquisition strategy employed by pathogens is the uptake of free iron. These mechanisms of uptake have been sparsely investigated due to the relative lack of freely available iron, however, some iron transporters have been identified. Gram-negative pathogens like *Legionella pneumophila* and, purportedly, some Gram-positive pathogens utilize the ferrous iron importer FeoAB for iron acquisition (62, 63). This system is regulated by Fur in Gram-

negative bacteria. Using transcriptional regulators like Fur enables bacteria to sense the bioavailability of iron and regulate iron acquisition systems accordingly.

In addition to iron acquisition genes, Fur regulates genes involved in virulence. In iron-limited conditions, Fur-mediated de-repression of transcription allows the production of secreted virulence factors. For example, *S. aureus* secretes hemolysins and cytotoxins which ultimately results in release of iron and iron sources thereby promoting bacterial survival and transmission (60).

Iron is indispensable for virtually all life forms, a fact that is aptly demonstrated by the impressive diversity of iron-requiring host processes. Bacterial pathogens also have a requirement for iron, and have evolved sophisticated mechanisms to overcome iron restriction. The host places tremendous importance on its ability to withhold iron (and other metals like zinc and manganese) from invading pathogens, in a process collectively referred to as nutritional immunity. These processes are discussed in the following sections.

1.3 Nutritional Immunity

Nutritional immunity refers to the processes whereby the host sequesters the availability of essential nutrients in order to combat the nutrient acquisition strategies of pathogens, curtail microbial growth and ultimately promote pathogen clearance (4). Transition metals like iron are not only essential for host biology but are also critical for microbial survival and replication. Therefore, in nutritional immunity, the sequestered nutrients consist largely of transition metals such as iron, manganese, and zinc. Further, the regulatory mechanisms used to reduce iron toxicity also play roles in nutrient restriction during bacterial infection.

1.3.1 Iron restriction in the host

The primary method of iron sequestration within the host is that most iron in the body is stored intracellularly complexed with other proteins. As discussed previously, ferrous iron is complexed with heme which is bound by hemoglobin in erythrocytes (64) and ferric iron is stored intracellularly bound by ferritin. However, many pathogens have

evolved effectors of erythrolysis such as the *Staphylococcus aureus* α -toxin which lyses red blood cells to release the large pool of stored iron (65). When this occurs the host uses glycoproteins like hemopexin and haptoglobin, which are circulating in the serum, to scavenge heme and hemoglobin, respectively (66). Another factor limiting iron availability to pathogens is the scarcity of free iron in the extracellular environment. This is due to iron being tightly bound to Tfn in circulation. Generally, Tfn levels are maintained so that approximately half of circulating Tfn is saturated. This allows immediate sequestration should free iron unexpectedly become available, such as from erythrolysis during infection.

At mucosal surfaces, the host utilizes the glycoprotein lactoferrin, produced by neutrophils and epithelial cells, to bind and therefore sequester ferric iron (67–69). Additionally, once at infectious foci, neutrophils release neutrophil gelatinase-associated lipocalin (NGAL, or Lipocalin 2) which binds to and sequesters bacterial catechol-type siderophores (70). Recall, siderophores are small, high-affinity ferric iron binding molecules secreted by bacteria that aid in bacterial iron acquisition. In addition to reducing iron availability via binding proteins, the host also utilizes transport mechanisms to alter iron distribution during infection.

1.3.2 NRAMP1

One mechanism of altering iron distribution during infection is the utilization of metal transporters to pump nutrients away from bacteria-containing compartments. One such transporter is the membrane protein natural resistance-associated macrophage protein 1 (NRAMP1). NRAMP1 was originally discovered due to the natural resistance expression of NRAMP1 provided during infection caused by the pathogens *Salmonella typhimurium*, *Leishmania donovani* and certain *Mycobacterium* species (71). NRAMP1 (encoded by the human gene SLC11A1) is an integral membrane protein that transports divalent cations (72). It is expressed primarily in professional phagocytes, particularly from the spleen and liver, but has recently been discovered to be expressed in lymphocytes as well (73). NRAMP1 localizes to late endocytic compartments within the cell and is specifically recruited to phagosomal membranes in macrophages (74, 75) where it works to extrude ions like Mn^{2+} , Zn^{2+} , and Fe^{2+} out of the phagosome lumen (76–78). This

action limits the availability of these essential nutrients to phagocytosed bacteria and controls bacterial infection.

1.3.3 DMT1

Another metal transporter implicated in nutritional immunity is the iron-transporting protein DMT1. DMT1 (also known as NRAMP2, DCT1, encoded by the human gene SLC11A2) is also a divalent cationic metal transporting protein with an unusually broad substrate range including Fe^{2+} , Zn^{2+} , Mn^{2+} , Co^{2+} , Cd^{2+} , Cu^{2+} , Ni^{2+} , and Pb^{2+} (28). As discussed previously (section 1.2.3), DMT1 is involved in iron uptake in the duodenum however it is also present at the plasma membrane, early and late endosomes in many cells types (79, 80). One recent study demonstrated that upon infection by uropathogenic *E. coli*, macrophages upregulate DMT1 expression at the plasma membrane which presumably results in increased iron uptake and therefore limits the availability of iron to extracellular *E. coli* (81). While the role of DMT1 in infection hasn't been studied extensively, considering the functional similarity of DMT1 to NRAMP1, it is likely that DMT1 also contributes to nutrient restriction during infection, particularly in cells that do not otherwise express high levels of NRAMP1.

1.3.4 Inflammatory hypoferremia

During infection the host regulates the production or activity of iron-related proteins to generate a hypoferremic environment within the body in a process called inflammatory hypoferremia (82). Induction of inflammatory hypoferremia is mediated by cytokines, such as interferon (IFN)- γ and interleukin (IL)-6, and hepcidin which are produced in response to infection. Increased hepcidin production results in increased degradation of Fpn thereby reducing export of iron into circulation, retention of iron intracellularly, and decreased availability of iron to extracellular bacteria. IFN- γ and IL-6 induce the acute phase response which results in increased production of iron-scavenging proteins such as lactoferrin, haptoglobin and ferritin (83), as discussed above. Hypoferremia during infection has long been recognized and investigated but more recently there has been renewed interest in nutritional immunity concerning other essential transition metals.

1.3.5 Manganese and zinc binding proteins

Like iron, other transition metals such as zinc and manganese play critical roles in host and bacterial processes. Among other enzymes, the enzyme superoxide dismutase requires manganese as a cofactor and is very important for resistance to oxidative stress for both the host and bacteria (84). Zinc is the second most abundant transition metal after iron in both the host and bacteria. It is critical in immune regulation, signal transduction and apoptosis in the host and plays important catalytic and structural roles in bacteria (85). As such, both manganese and zinc are also important targets for nutritional immunity (86).

One of the key mediators of zinc restriction and the only known chelator of manganese is calprotectin (CP) (87). CP is a heterodimer consisting of the proteins S100A8 and S100A9: both members of the S100 family of calcium-binding proteins. The antimicrobial activity of CP is mediated by binding of calcium to S100A8 and S100A9. Calcium binding induces conformational changes in the proteins allowing high affinity binding to either one manganese atom or two zinc atoms at the interface of the two subunits (88). CP is abundant in the cytoplasm of neutrophils and is released at the site of infection via degranulation and neutrophil extracellular traps (NETs). As neutrophils are the first responders to sites of infection, CP plays an important role in the immediate defense against invading pathogens. Specifically, CP displays dose-dependent antimicrobial activity against *S. aureus* in a tissue abscess model (89) and also is the key mediator of the antifungal properties of NETs (90, 91).

Other members of the S100 family of proteins include S100A7 (also known as psoriasin) and S100A12 (also known as calgranulin C and EN-RAGE). S100A7 is a protein found on healthy human skin that mediates killing of *E. coli* via sequestration of zinc (92). S100A7 production is enhanced in hyperproliferative skin diseases such as psoriasis and has also been implicated in strengthening epithelial tight junctions. This presumably enhances skin innate barrier function by impeding the entrance of invasive microbes (93). S100A12 is yet another zinc chelating protein produced by neutrophils and has been shown to have antibacterial effects against *Helicobacter pylori* (94), and *Listeria monocytogenes* and also antifungal effects against *Candida albicans* (95).

CP, S100A7, and S100A12 each bind zinc and while this seems functionally

redundant it serves to highlight the importance of zinc limitation during infection. Further, since both CP and S100A12 are housed in neutrophils and released at the site of infection, it has been proposed by Cunden *et al* (2016) that S100A12 chelates a portion of the zinc pool to allow more CP molecules to bind to manganese (95). In addition to iron, manganese, and zinc, copper is another transition metal implicated in nutritional immunity. However, copper distribution seems to be altered in a manner opposite to that of the transition metals already discussed.

1.3.6 Copper transporting proteins

Just like the previous transition metals discussed, copper is a critical component of proteins involved in many cellular processes and at high concentrations has toxic effects. In fact, the toxic and therefore antimicrobial properties of copper have long been known and exploited *ex vivo*. Copper is used in plumbing for its antimicrobial properties (96, 97) and currently there is interest in using copper on hospital surfaces to reduce occurrence of nosocomial infections (98). Due to these properties, copper also plays a role in nutritional immunity.

However, in contrast to the withholding mechanisms used for iron, manganese, and zinc, evidence has emerged that the host specifically utilizes copper to exert an antimicrobial effect on invading pathogens. In response to pro-inflammatory stimuli IFN- γ and LPS, macrophages upregulate expression of CTR1 and ATP7A (99). Both CTR1 and ATP7A are copper-transporting proteins. CTR1 (SLC31A1) functions at the plasma membrane of macrophages as a copper importer (100). Conversely, ATP7A is copper transporter localized to both the plasma membrane where it exports copper and also to endocytic compartments within the cell where it pumps copper into intracellular vesicles (101). During inflammation, cellular copper uptake is increased, presumably through CTR1, and the copper binding protein ATOX1 shuttles copper to ATP7A (102). ATP7A then pumps copper into phagosomes for intoxication of phagocytosed bacteria. Accumulation of copper within the phagosome has been shown to have bactericidal effects against *E. coli* (99) and *M. tuberculosis* deficient in copper efflux (103).

1.4 Ferroportin

1.4.1 Function and structure

Another metal transporter implicated in nutritional immunity and of particular interest to this study is Fpn. Ferroportin (also known as SLC40A1, IREG1 and MTP1) is the only known mammalian iron-exporting protein (34–36) and is part of the major facilitator superfamily (MFS) of transporting proteins. In addition to iron transport, Fpn has recently been shown to have cobalt, zinc, and manganese transport activity as well (104, 105). Fpn is expressed in tissues involved in iron homeostasis, namely duodenal enterocytes, hepatocytes, and macrophages where it plays a role in iron absorption, storage, and recycling, respectively (106). Fpn is also critical during fetal development for transporting iron through the placenta to the fetus as demonstrated by the non-viability of mice lacking Fpn (107).

Fundamental information about the structure of Fpn has been controversial. Certain groups described the topology of Fpn with either one or both of the N- and C-termini to be extracellular (108, 109) while others described either one or both of the N- and C-termini to be intracellular (110, 111). Further, the number of transmembrane domains Fpn contains was debated, with groups predicting the presence of either ten (36) or twelve (110) transmembrane domains. However, several models based on other MFS transporters with twelve transmembrane domains suggest that both termini of human Fpn are intracellular (112–114). Moreover, Taniguchi *et al* (2015) (115) used a putative bacterial homologue of Fpn from *Bdellovibrio bacteriovorus* to obtain crystal structures revealing two 6-helix bundles characteristic of the MFS proteins (116). The structures revealed two states: an inward and outward facing state in which a cleft, presumably the metal binding site, is exposed to the inside or outside of the cell, respectively.

1.4.2 Mechanism of iron binding and transport

While the mechanism of iron binding and transport hasn't been determined conclusively, some information is known. Within the cell, PCBP2 (mentioned in 1.2.4) shuttles ferrous iron to Fpn for export (33, 117). Beyond this, the actual molecular mechanism of iron transport by Fpn remains largely unknown due to difficulties in crystallizing the human

protein. Based on the crystal structures from the bacterial homologue, Taniguchi *et al* (2015) (115) propose that in human Fpn, the iron atom is coordinated by one asparagine, one aspartic acid and two serine residues. They also propose a model of the transport cycle in which iron binding results in conformational changes in the alpha-helices from the inward to the outward facing state thereby facilitating export. It has also been proposed that once outside the cell, ceruloplasmin is responsible for oxidizing ferrous iron to ferric iron to allow binding to Tfn (118). However, it still has not been conclusively determined what form of iron Fpn transports or if there is antiporter or symporter activity associated with Fpn. Further investigation is required confirm the proposed mechanism of transport (115) .

1.4.3 Ferroportin regulation

Fpn has many mechanisms of regulation that allow for differential expression between different tissues. Fpn is regulated transcriptionally based on the presence of heme. Heme causes the degradation of the repressor Bach1 which in turns allows transcription to occur via Nrf2 (119, 120). Additionally, the production of NO acts to up-regulate Fpn expression also using Nrf2-mediated transcription (121).

Fpn expression is regulated at the translational level using the iron-responsive element (IRE) located at the 5' untranslated region of Fpn mRNA. Under conditions of iron deficiency, iron-responsive proteins (IRP) bind to IREs and cause translational repression (122).

Further, Fpn is regulated post-translationally by the hormone hepcidin. Recall, hepcidin is a small peptide produced by the liver that regulates intestinal iron absorption and iron recycling by macrophages (39, 123). During inflammation, hepcidin is produced and binds to Fpn thereby causing its internalization and subsequent degradation (38, 107, 124). The mechanism of hepcidin-mediated degradation of Fpn occurs as follows: hepcidin binds to Fpn, which is then ubiquitinated and internalized (124) and subsequently shuttled through the multivesicular body pathway (125) for degradation by the lysosome (38).

1.4.4 Ferroportin-related diseases

Since Fpn plays a central role in iron homeostasis it follows that misregulation of Fpn expression or changes in Fpn function can lead to disease. Mutations in the gene encoding Fpn result in HH type 4, sometimes referred to as Fpn disease. Reported mutations in Fpn are heterogeneous but, despite the heterogeneity, the diseases typically present as one of two phenotypes (126). Some mutations result in a “gain-of function” phenotype in which Fpn is resistant to hepcidin leading to increased absorption of dietary iron, oversaturation of plasma Tfn, and ultimately iron overload (127). This disease more closely resembles the other HH discussed in section 1.2.5.

Alternatively, some mutations lead to a loss-of-function phenotype in which iron export via macrophages is reduced (128). This disease presents with iron overload in macrophages, increased serum ferritin concentrations but normal Tfn saturation. It is presumed that even though macrophages ultimately become iron over-loaded, because they have an extensive repertoire of mechanisms to deal with reactive oxygen species the iron-overload is not extensively pathogenic. Thus, this form of Fpn disease does not seem to cause clinically important damage.

1.4.5 Ferroportin and infection

Fpn is also important during infection. As discussed, hepcidin production is up-regulated during infection resulting in Fpn degradation and cellular iron retention. Cellular iron retention is crucial to restricting infection by the extracellular, iron-dependent pathogen *Vibrio vulnificus* (82). Mice lacking hepcidin, in which Fpn export is unrestricted, were significantly more susceptible to infection compared to WT mice. Further, mouse survival was restored upon supplementation with hepcidin peptides demonstrating the importance of Fpn during infection with extracellular bacteria.

Another facet of investigation is the role of Fpn during infection with intracellular pathogens, especially concerning macrophages. For instance, macrophages infected with *S. typhimurium* have increased Fpn mRNA expression indicating macrophages increase iron export during *S. typhimurium* infection (129). This directly contrasts the observed hepcidin-mediated cellular iron retention in hypoferremia of inflammation. Similarly, in macrophages infected with WT *L. monocytogenes*, Fpn mRNA levels significantly

increased compared to the static Fpn mRNA levels observed in cells infected with a strain defective in phagosome escape (130). The increase in Fpn expression corresponded to decreased bacterial CFUs and conversely, treatment with hepcidin lead to increased bacterial CFUs. Further, Fpn over-expression in macrophages has been demonstrated to limit intracellular growth of *M. tuberculosis*, presumably by restricting iron availability to the pathogen (131). Interestingly, it has also been reported that Fpn is rapidly recruited to *M. tuberculosis*-containing phagosomes where it would presumably provide iron to the phagocytosed bacteria (132).

1.5 Phagocytes

Phagocytes play a key role in innate immunity owing to their role in nutritional immunity. However, phagocytic cells also utilize mechanisms other than nutritional immunity as part of their role in the innate immune system which are reviewed in the following sections. Phagocytes include cells like neutrophils, dendritic cells and macrophages – the latter of which are the focus of this project.

1.5.1 Macrophages

Macrophages are major effectors of both the innate and adaptive immune response. The designation of a macrophage as a professional phagocyte is central to its contribution to innate immunity. What differentiates professional phagocytes like macrophages, neutrophils, and dendritic cells, from other cells is their exceptional efficiency in performing phagocytosis and also their large repertoire of receptors that confer phagocytic function and recognition of many PAMPs (133, 134). During inflammation, monocytes, the precursor to macrophages, are recruited from the circulation via chemoattractants. For example, in response to pro-inflammatory cytokines many cells express CCL2 which is a ligand for CCR2 found on monocytes that mediates recruitment (135). Following chemoattraction, monocyte recruitment in response to inflammation is thought to follow a similar mechanism to that of leukocyte extravasation during which rolling adhesion, tight adhesion – both mediated by selectins and integrins – and finally tissue translocation, occur (136). Once they have entered the inflamed tissue, monocytes

differentiate into active macrophages with different phenotypes depending upon environmental cues they receive. Further, activated macrophages fit into a spectrum of macrophage polarization states. On one end of the spectrum is the M1 classically-activated macrophage induced by PAMPs and inflammatory cytokines (IFN- γ) (137). At the other is the M2 alternatively-activated macrophage induced by anti-inflammatory cytokines like IL-10 and IL-4 (137). The M1 polarization state defines a pro-inflammatory, antimicrobial macrophage whereas the M2 macrophage is anti-inflammatory and is involved in tissue remodeling and repair (138, 139).

Macrophages are constantly sampling the environment using cytoplasmic extensions called filopodia (140). Constant environmental surveillance coupled with expression of a wide variety of phagocytic receptors allows macrophages to detect many signals ranging from apoptotic cells to pathogens. Once these signals are detected, macrophages initiate internalization of the recognized particle in a process termed phagocytosis.

1.5.2 Phagocytosis and phagocytic receptors

Phagocytosis is a receptor-mediated process whereby professional phagocytes, such as macrophages, internalize large particles into a membrane-bound vesicle called the phagosome (141). As mentioned above, the expression of a vast array of receptors allows macrophages to recognize a multitude of ligands. For example, Fc γ receptors recognize the Fc portion of human IgG found on opsonized particles or dectin-1, a PRR which recognizes fungal polysaccharides (142, 143). In contrast to these receptors is the integrin Mac-1 (also known as CR3 or $\alpha_M\beta_2$) which acts very promiscuously and recognizes over 30 ligands ranging from foreign particles to apoptotic corpses (141). It is important to note the fluidity of the plasma membrane of phagocytes which allows lateral movement of phagocytic receptors. Once a receptor is engaged, the now stationary ligand causes clustering of additional receptors which in turn activates the receptor to initiate phagocytosis (144). For example, Fc γ receptor clustering brings cytosolic domains – the immunoreceptor tyrosine-based activation motif (ITAM) – in close proximity which allows for phosphorylation of the ITAM motif and initiation of downstream signaling (134, 141).

1.5.3 Phagosome maturation

Once phagocytosis is initiated, the particle gets internalized into a membrane-bound compartment termed the phagosome. Newly formed phagosomes undergo a strictly ordered maturation process through membrane fusion events beginning with fusion of nascent phagosomes and early endosomes. This body, termed the early phagosome, further matures by sequential fusion with late endosomes and lysosomes, giving rise to late phagosomes and phagolysosomes, respectively (141).

The stage of phagosome maturation is defined by the phagosomal membrane composition which is altered through vesicular traffic to and from the phagosome. In Figure 1 (modified from (5)), a schematic outlining molecular markers that biochemically define the stages of phagosome maturation is presented. To begin, in the forming phagosome both phosphatidylinositol-3,4,5-trisphosphate [PI(3,4,5)P₃] and phosphatidylinositol 4-phosphate [PI(4)P] are enriched at the base of the phagocytic cup until the phagosome seals and membrane scission occurs (145, 146). After sealing, PI(3,4,5)P₃ is rapidly lost. In addition, phagosomes become enriched with phosphatidylinositol-3-phosphate [PI(3)P], a marker of early phagosomes, and this is accompanied by loss of PI(4)P (147). Another marker of early phagosomes is the Rab GTPase Rab5. Rab GTPases are important effectors in a variety of processes inside the cell including the regulation of membrane trafficking and alternate between active-GTP bound and inactive GDP-bound states. Rab5 accumulates on the nascent phagosome and facilitates fusion with early endosomes (148). In addition, it is required for the acquisition of Vps34 which is a phosphatidylinositol-3-kinase (PI3K) responsible for the conversion of phosphatidylinositol (PI) to PI(3)P and is therefore crucial to phagosome maturation (147).

Eventually the early phagosome transitions into a late stage phagosome upon acquisition of Rab7, the concomitant loss of Rab5, and regeneration of PI(4)P (146, 148). As well, the late phagosome is characterized by the acquisition of lysosome-associated

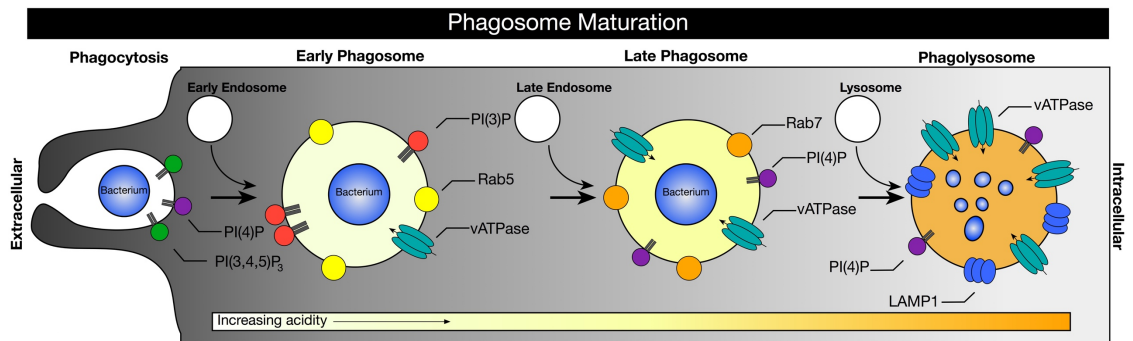


Figure 1. Phagosome maturation. The process of phagosome maturation involves a series of membrane fusion events that alter phagosome membrane composition and ultimately produce a mature, antimicrobial, phagolysosome. Shown are a number of membrane markers used to identify the phagosome stage such as PI(3)P, Rab5, Rab7, and LAMP1. Modified from (5).

membrane protein 1 (LAMP1). LAMP1 is an integral membrane protein found on late endosomes, lysosomes and fully mature phagosomes (149). The late endosome, as defined by the presence of LAMP1 and Rab7, then fuses with lysosomes to form the phagolysosome - the ultimate microbicidal compartment inside the cell. The phagolysosome can be defined biochemically by its markedly acidic pH and also by the presence of lysosomal hydrolases.

1.5.4 Antimicrobial effectors of macrophages

Phagosome maturation ultimately leads to the creation of a microbicidal organelle where killing is mediated through a number of mechanisms, namely: acidification, the use of degradative enzymes, reactive oxygen and nitrogen species, and nutrient limitation (5, 150). Phagosome acidification begins early in phagosome maturation with accumulation of vacuolar ATPases (vATPases) that pump H⁺ ions into the phagosome lumen (151). Low pH maintenance is also aided by the reduced proton permeability of the phagosome membrane, effectively reducing “proton leak” (151). Acidification is necessary for maturation and aids in pathogen clearance by creating a harsh environment for bacteria to survive.

In addition to acidification, lysosomal proteases are delivered to the phagosome and are active against phagocytosed bacteria. A prominent example is the cathepsin family of cysteine proteases that generally become active at lysosomal pH and promote killing of the bacteria (152, 153). To add to this already hostile environment, the macrophage also uses NADPH oxidase to produce reactive oxygen and nitrogen species that damage proteins, lipids and DNA (154). Lastly, as already discussed in detail above, macrophages utilize nutritional immunity to augment the other antimicrobial effectors of the phagosome. By far the most extensively studied example is the NRAMP1 protein which is recruited to the phagosome and acts to extrude divalent cations from the lumen of the phagosome (75).

1.5.5 Bacteria that manipulate phagocytosis

Remarkably, despite numerous mechanisms employed to kill phagocytosed bacteria, many pathogens have evolved ways to survive inside macrophages. Some intracellular

pathogens like *Yersinia pestis* are capable of altering phagosome maturation by subverting acidification thereby effectively evading killing by macrophages (155). Similarly, the pathogen *Klebsiella pneumoniae* alters phagosome maturation, prevents delivery to the lysosome and thereby mediates survival within the macrophage (156). *M. tuberculosis* uses many mechanisms to halt phagosome maturation (157–159) and also prevents inflammasome activation to mediate survival within the macrophage (160). Bacterial toxins have also been used to escape the phagosome. This method is employed by *L. monocytogenes* which produces the toxin Listeriolysin O, a pore-forming toxin that disrupts the membrane of the phagosome to mediate escape into the macrophage cytoplasm (161).

1.6 Endocytosis and endocytic protein trafficking

Another important aspect to review for this study are endocytic protein trafficking pathways. Endocytosis is broad term encompassing several different pathways including phagocytosis and a slightly different process, receptor-mediated endocytosis. As already discussed, phagocytosis involves the receptor-mediated internalization of large particles such as apoptotic cells and microbes. Receptor-mediated endocytosis involves the selective uptake of specific molecules, such as Tfn or epidermal growth factor (EGF), bound to their cognate membrane-embedded receptors into a membrane bound compartment, or endosome (162). Endosomes undergo a similar maturation process as outlined for the phagosome in section 1.5.3. This similarity highlights that despite differences in cargo and in initialization of internalization, internalized proteins ultimately join the endocytic protein trafficking network within the cell. However, while the final step in phagocytosis is always the destruction of the internalized cargo, during endocytosis some cargos have fates besides destruction. Both the final fate of trafficked cargo and the trafficking mediators involved define different trafficking pathways. The following briefly reviews indispensable mediators of protein trafficking, the Rab GTPases, and some fates of endocytosed cargo.

1.6.1 Rab GTPases

Rab GTPases are important effectors of vesicular, and therefore protein trafficking (163). In humans, there are more than 60 identified Rabs that are localized to distinct intracellular membranes (164). Thereby, Rabs are important for defining the identity of an endocytic vesicle but also for regulating membrane traffic throughout the cell. Rab GTPases function as “molecular switches” in that they alternate between active-GTP bound and inactive GDP-bound states. This cycle is mediated by both GEFs (guanine nucleotide exchange factors) and GAPs (GTPase activating proteins). GEFs facilitate the exchange of GDP and GTP, while GAPs are important for catalysis of GTP hydrolysis. Molecular switching allows Rab proteins to regulate endosomal membrane trafficking mechanisms such as receptor recycling or receptor degradation.

1.6.2 Recycling

One important fate for endocytosed cargo is recycling back to the plasma membrane. TfnR is considered a prototypical recycled protein. When Tfn binds to TfnR, this complex is internalized via receptor-mediated endocytosis. As with the phagosome, the endosome begins to acidify resulting in the dissociation of ferric iron from Tfn, allowing iron to be transported to the cytoplasm (165). The apoTfn-TfnR complex is eventually recycled back to the plasma membrane via one of two routes: the fast or the slow recycling pathway (162). The fast route is mediated by the GTPase Rab4 and involves direct transport from the early endosome back to the plasma membrane (166). Alternatively, the slow route is mediated by Rab11 and involves sorting the complex into the perinuclear endocytic recycling compartment (ERC) from which the complex is recycled back to the plasma membrane (167). At the plasma membrane, the neutral pH decreases the affinity of TfnR for apo-Tfn resulting in release of apo-Tfn into the circulation. Because TfnR recycles through both pathways, it is often used as a tool to investigate the trafficking mechanism of other proteins.

1.6.3 Degradation

Not all endocytosed proteins end up being recycled. For instance, if a cell needs to stop signaling from a certain ligand the cell then degrades the ligand’s receptor. Such is the

case for the epidermal growth factor (EGF) and its receptor (EGFR) which is degraded via the formation of multivesicular bodies (MVBs) (168). Upon binding to EGF, the EGF-EGFR complex is endocytosed into clathrin-coated vesicles. The clathrin-coat is shed and this vesicle fuses with the early endosome. EGFR is then sorted into intraluminal vesicles (ILVs) which are invaginations of endosomal membrane into the lumen of the endosome (169). This sorting is mediated by the endosomal sorting complex required for transport (ESCRT) machinery. Endosomes containing ILVs are termed MVBs. Upon fusion of the MVB with the lysosome, any cargo contained within the ILVs is degraded (170). As with recycling, Rab proteins mediate some aspects of the MVB pathway. For example, Rab7 is important for fusion of MVBs with lysosomes wherein RNA interference of Rab7 resulted in enlarged MVBs and almost complete inhibition of EGFR degradation (171).

1.7 Project rationale and hypothesis

Nutritional immunity is an important facet of innate immunity. During bacterial infection, macrophages are key mediators of the nutritional immune response, especially iron sequestration. Ferroportin is an iron-exporting protein found on the plasma membrane of macrophages that plays a role in nutritional immunity. While the mechanism and fate of hepcidin-induced Fpn degradation is characterized, this project is focused on the fate and trafficking mechanism exclusively of phagosomal Fpn during bacterial infection. More specifically, in the early stages of infection - before increased production of hepcidin occurs - what happens to Fpn during phagocytosis of bacteria? If the localization or function of Fpn was not altered in any way (Fig 2A), upon phagosome formation Fpn would remain on the phagosomal membrane (Fig 2B). Due to the orientation of Fpn in the membrane, this would ultimately lead to the transport of iron into the phagosomes and provision of phagocytosed bacteria with iron.

I hypothesized that during phagocytosis, macrophages remove Fpn from the phagosomal membrane to prevent the extrusion of iron into the phagosome lumen.

As depicted in Figure 2, several mechanisms employed by the macrophage could remove Fpn from the phagosome: i) Fpn may be retrieved from phagosomes and

trafficked back to the plasma membrane through recycling pathways akin to TfnR (172) (Fig 2E), ii) regions of the polypeptide in the phagosome lumen may be proteolytically degraded while it remains in the phagosomal membrane upon phagosome-lysosome fusion (Fig 2D), or iii) it may be degraded entirely in the phagosome lumen as part of a MVB akin to the EGFR (168) (Fig 2C). Lastly, it is possible that Fpn gets caught in the cytoskeletal network of the cell and is excluded from the phagosome altogether (Fig 2F), akin to CD45, a receptor-like protein tyrosine phosphatase (173).

To test this hypothesis, I pursued three different objectives. 1) The first objective was to determine if Fpn is removed from the phagosome during phagocytosis using fluorescent fusion proteins and fluorescence microscopy. 2) The second objective was to determine if Fpn is removed from the phagosome via degradation using an inhibitor of cellular degradation mechanisms. 3) Lastly, I wanted to compare Fpn localization to known trafficking mediators within the cell to determine the trafficking mechanism of Fpn from the phagosome.

The goal of this research is to advance our understanding of iron-restriction during bacterial infection and help provide a more complete understanding of host nutritional immune responses.

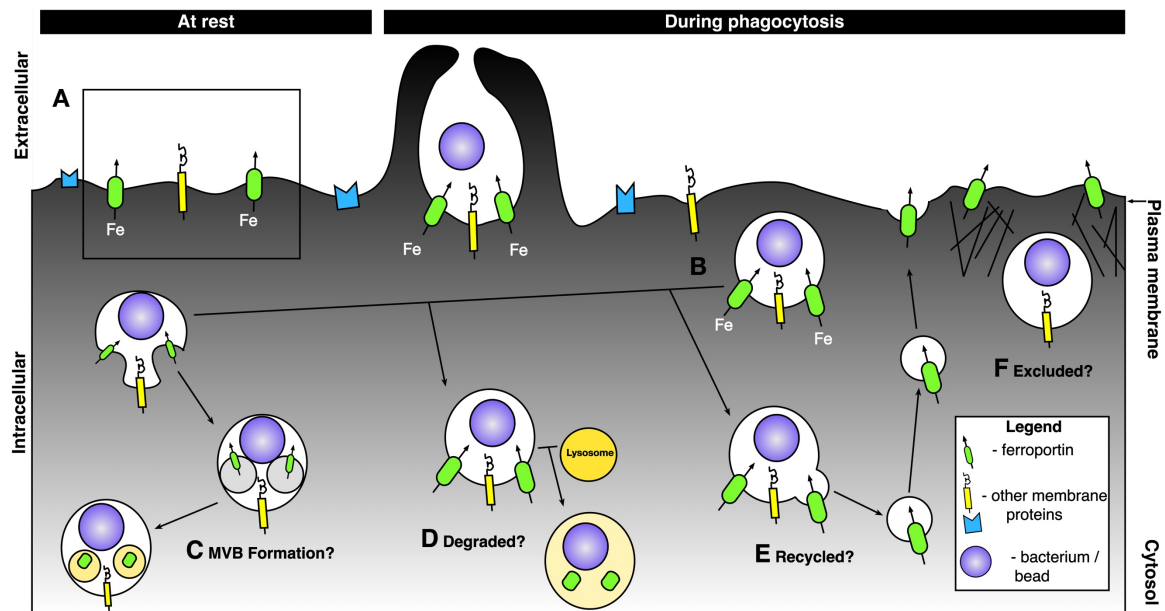


Figure 2. Postulated mechanisms of Fpn removal from the phagosome. (A) At rest, Fpn resides in the macrophage plasma membrane where it extrudes iron out of the cell. If Fpn is not modulated, after phagocytosis of a bacterium, Fpn would extrude iron into the phagosome lumen providing iron that could be used for microbial growth **(B)**. In **(C)**, Fpn is removed from the phagosome membrane and subsequently degraded via the formation of a MVB. Fpn may also remain on the phagosomal membrane and get proteolytically degraded after fusion with a lysosome **(D)** or it may be removed from the phagosome membrane and then be recycled back to the plasma membrane **(E)**. Lastly, it is possible that Fpn gets trapped in the cytoskeletal network of the cell and is excluded from the phagosome altogether **(F)**.

CHAPTER 2 – MATERIALS and METHODS

2.1 Reagents

Roswell Park Memorial Institute 1640 medium (RPMI) and fetal bovine serum (FBS) were from Wisent Inc (St. Bruno, QC, Canada). Paraformaldehyde 16% solution and #1 thickness round cover glass slips (18mm diameter) were from Electron Microscopy Sciences (Hatfield, PA, USA). The Cell Proliferation Dye eFluor® 670 was from eBiosciences (San Diego, CA, USA). Both 3.14µm and 1.54µm silica beads were from Bangs Laboratories (Fishers, IN, USA). Lyophilized human IgG was from Sigma Aldrich (St. Louis, MO, USA). Rat anti-mouse LAMP-1 antibody (clone 1D4B) was deposited by J.T August to The Developmental Studies Hybridoma Bank at the University of Iowa (Iowa City, IA, USA). The pharmacological agents LY294002 and Concanamycin A were from Santa Cruz Biotechnology (Dallas, TX, USA). Fluorophore conjugated antibodies including goat anti-rat Cy3 and goat anti-human AlexaFluor® 647 were from Jackson ImmunoResearch (West Grove, PA, USA). Lipofectamine® 3000 and LysoTracker® Red DND-99 were from Invitrogen (Mississauga, ON, Canada). Horse serum was from Sigma-Aldrich (St. Louis, MO, USA). All restriction enzymes were purchased from New England Biolabs (Ipswich, MA, USA).

2.2 Bacterial strains, plasmids and culture conditions

The bacterial strains and plasmids used in this study are summarized in Table 1. Methicillin-resistant *S. aureus* strain USA300, cured of its endogenous antibiotic resistance plasmid, was routinely cultured in Tryptic Soy broth (TSB) (Difco) at 37°C with shaking. When appropriate, *S. aureus* carrying the plasmid pAH9 was cultured in TSB in the presence of erythromycin at 3 µg/mL. Solid media were prepared with the addition of Bacto-agar (1.5% w/v).

For cloning purposes, *E. coli* DH5α was cultured in LB broth with shaking or on LB agar (1.5% w/v) at 37°C. *E. coli* carrying the plasmid encoding Fpn-GFP (called pTF1) was grown at 30°C for 48h. Throughout this study, all *E. coli* strains carrying plasmids were cultured in media containing kanamycin (40 µg/mL).

Table 1. Bacterial strains and plasmids used in this study

Strain or plasmid	Description*	Source / Reference
<i>Staphylococcus aureus</i>		
USA300	USA300 LAC; MRSA cured of antibiotic resistance plasmid	Laboratory stock
<i>Escherichia coli</i>		
DH5a	F- ϕ 80 dlacZ Δ M15 recA1 endA1 gyrA96 thi-1 hsdR17(rK- mK+) supE44 relA1 deoR Δ (lacZYA-argF) U169 phoA λ -	Laboratory stock
Plasmids		
pAH9	<i>S. aureus</i> expressing mCherry from constitutive <i>sarA</i> promoter; Ery	(174)
pTF1	Mammalian expression vector encoding human Fpn fused to GFP; Kan	This study
mCherry-TfnR	Mammalian expression vector encoding full length human TfnR fused to mCherry; Kan	Michael Davidson Addgene#55144
GFP-Rab4	Mammalian expression vector encoding Rab4 fused to GFP; Kan	J. Brumell
pTF2	Mammalian expression vector encoding human Fpn fused to mRuby; Kan	This study
TfnR-GFP	Mammalian expression vector encoding TfnR fused to GFP; Kan	S. Grinstein
2xFYVE-RFP	Mammalian expression vector encoding tandem FYVE domains fused to RFP; Kan	S. Grinstein
Rab5WT-mCherry	Mammalian expression vector encoding Rab5 fused to mCherry; Kan	R. Flannagan
Rab5CA-mCherry	Mammalian expression vector encoding constitutively active Rab5 (Q79L) fused to mCherry; Kan	R. Flannagan
p-mCherry-N1	Mammalian expression vector encoding soluble mCherry; Kan	Clontech
Rab7-mCherry	Mammalian expression vector encoding Rab7 fused to mCherry; Kan	(175)

* Abbreviations: Ery and Kan indicate resistance to erythromycin and kanamycin respectively

The plasmid carrying the human Fpn (SLC40A1) gene (plasmid ID HsCD00335917) was purchased from the Harvard Plasmid Repository, Harvard University. To generate a plasmid encoding a Fpn-GFP fusion protein, the Fpn gene was PCR-amplified using the primers Fpn-F and Fpn-R (see Table 2 for primer sequence) and HsCD00335917 as a template. The amplicon was cloned into the mammalian GFP expression vector pEGFP-N1 (Clontech) using *EcoRI* and *AgeI* restriction digest enzymes. The resulting Fpn-GFP expression vector, called pTF1, was identified by PCR and restriction analysis and confirmed by DNA sequencing at the London Regional Genomics Center (Robarts Research Institute, The University of Western Ontario).

To generate a plasmid encoding a Fpn-mRuby fusion protein, Fpn-F and Fpn-R primers (Table 2) were used to PCR amplify the Fpn gene using pTF1 as the template. The amplicon was cloned into the mammalian mRuby expression vector mRuby-N1 (a gift from Michael Davidson, Addgene #54581) using *EcoRI* and *AgeI* restriction digest enzymes. The resulting vector, called pTF2, was confirmed by DNA sequencing.

Table 2. Oligonucleotides used for cloning

Name	Sequence*
Fpn-F	5' ATATATTGAATTCATGACCAGGGCGGGAGATCACAAC 3'
Fpn-R	5' ATATATTACCGGTGCAACAACAGATGTATTTGCTTGA 3'

Used for cloning Fpn-GFP and Fpn-mRuby

* restriction sites are underlined

2.3 Mammalian cell culture and transfection

The murine macrophage cell line RAW264.7 (RAW) was obtained from the American Type Culture Collection (ATCC, Manassas, VA, USA) and grown in RPMI 1640 containing 10% FBS (v/v) at 37°C in a humidified atmosphere containing 5% CO₂. Transfection was performed using Lipofectamine® 3000 as per the manufacturer's protocol. Briefly, cells were seeded onto 18mm glass coverslips and incubated at 37°C with 5% CO₂ overnight. In 125µL serum-free (SF) RPMI, 1µg of plasmid DNA was mixed with 2µL P300 reagent and 2µL Lipofectamine reagent, incubated for 5min, and then added dropwise to 1 well of a 12-well tissue culture plate. After at least 6h incubation with Lipofectamine/DNA mixture, cells were rinsed with SF-RPMI and incubated overnight with RPMI containing 10% FBS (v/v).

2.4 Silica bead opsonization and phagocytosis

Silica beads were opsonized with human IgG (1 mg/mL) for 1 hr in PBS at room temperature with constant shaking. After washing, IgG-coated beads were added to individual wells containing transfected RAW cells cultured on 18-mm glass coverslips and centrifuged for 1 min at $177 \times g$ to promote synchronization of phagocytosis. Plates were then incubated at 37°C with 5% CO₂ for various time-points and, at the appropriate time, cells were washed with PBS and fixed with 4% (v/v) paraformaldehyde (PFA) for 20 min at room temperature.

For all *S. aureus* infections, the bacteria were diluted in SF-RPMI and added to RAW cells at a multiplicity of infection of 30. Synchronization of engulfment and processing of cover slips after infection were performed as described above.

Detection of extracellular beads was performed by staining for 10 min with fluorophore-conjugated secondary anti-human antibodies (0.8 µg/mL in PBS) after fixation.

2.5 Immunofluorescence staining of LAMP1

RAW macrophages cultured on 18-mm glass coverslips and transfected with pTF1 were exposed to either IgG-coated silica beads or eFluor670-labelled *S. aureus* USA300. eFluor labelling of bacteria was done in saline containing 5 µM eFluor670 dye for 10

min. Bacteria were then washed with saline and re-suspended in SF-RPMI for infections. Phagocytic targets were added to macrophages as describe above and at 1 hr post-addition the cells were fixed with 4% (v/v) PFA at room temperature for 20 min. Cells were then permeabilized using ice-cold methanol for 3 min. Permeabilized cells were blocked for at least 4 hr using horse serum. Next, the rat anti-mouse LAMP1 antibody (1:100 dilution of hybridoma supernatant) diluted in blocking buffer was incubated with the cells for at least 1 hr. Cells were then washed with PBS and the primary antibody detected using a goat anti-rat Cy3 antibody (750 µg/mL in blocking buffer). After 30 min with secondary antibody, cells were washed thoroughly with PBS and imaged using laser-scanning confocal microscopy.

2.6 Concanamycin A treatment and Lysotracker® loading of macrophages

For inhibition of vATPase-mediated acidification, RAW cells seeded on 18-mm glass coverslips and transfected with pTF1 were pre-treated with Concanamycin A (500 nM in SF-RPMI) for 30 min. IgG-coated beads were added to the cells, as described above, and then fixed 30 min after addition of beads. To demonstrate the effectiveness of Concanamycin A, untransfected RAW cells pre-treated with 500 nM Concanamycin A as above were incubated with Lysotracker® Red DND-99 at a final concentration of 250 nM (diluted in SF-RPMI) for 10 min. Cells were then washed 3 times with SF-RPMI and immediately imaged live by wide-field microscopy.

2.7 Wide-field fluorescence microscopy

Wide-field fluorescence and differential interference contrast microscopy were performed on a Leica DMI6000B inverted microscope equipped with 40x (NA 1.3), 63x (NA 1.4) and 100x (NA 1.4) oil immersion PL-APO objectives, a Leica 100W Hg high-pressure light source and the Hammamatsu Orca Flash 4.0 and Photometrics Evolve 512 Delta EM-CCD cameras. This microscope is also outfitted with an objective warmer and an enclosed heated stage insert with CO₂ reperfusion (Live Cell Instruments) for live cell fluorescence imaging. Images were acquired with 100x objective with the Photometrics EM-CCD camera using FITC, Cy3 and Cy5 filter settings as appropriate. All images

were obtained using wide-field fluorescence microscopy and subsequently deconvolved as described in section 2.9 unless otherwise indicated.

2.8 Confocal microscopy

Laser scanning confocal fluorescence microscopy was performed on a Leica TC5 SP5 microscope comprised of a DMI6000 CS inverted microscope outfitted with argon/2 (458, 476, 488, 514 nm), HeNe1 (543 nm), HeNe2 (633 nm) lasers and a PL-APO 63x oil immersion objective (NA 1.4). This microscope is equipped with triple dichroic TD 488/543/633, a DD 488/543 dichroic and a tunable Acousto-Optical Beam Splitter for all laser lines. All confocal imaging was performed at the Robarts Research Institute Imaging Facility (The University of Western Ontario).

2.9 Deconvolution and image analysis

Z-stacks obtained using wide-field microscopy were subsequently deconvolved using the iterative 3D deconvolution application of the Leica Application Suite software prior to image analysis. All images were analyzed using ImageJ (National Institutes of Health, Bethesda, MD) and illustrations prepared using AutoDesk® Graphic.

For quantification of Fpn-positive phagosomes a set of criteria was followed. First, only cells that expressed Fpn-GFP at the plasma membrane were analyzed as this was indicative that Fpn was being trafficked correctly throughout the cell. Further, only entirely intracellular phagocytic targets (the target did not label with anti-human secondary antibody, see section 2.4) were counted. For a phagosome to be considered Fpn-positive there had to be distinct signal defining the phagosome of similar intensity to the plasma membrane, it had to encircle at least 50% of the phagosome, and span more than 1 layer of the z-stack.

Co-localization analysis was performed using either the JACoP plugin or the Co-loc2 plugin on ImageJ. JACoP was used to calculate Mander's Coefficient and Pearson's Coefficient for Figure 7 and Figure 11, respectively. To calculate Mander's Coefficient: GFP-Rab4a was set to Ch1 and the corresponding mCherry was set to Ch2, the threshold was set manually and 3 slices per stack were used to calculate Mander's Coefficient for each cell. M1 is the value presented as M2 is confounded by the plasma membrane

populations of mRuby-Fpn and mCherry-TfnR. Pearson's Coefficient was calculated by setting Fpn-GFP to Ch1 and Rab5-mCherry to Ch2 and using the average of 3 slices per stack to calculate Pearson's Coefficient for each cell.

Co-loc2 was used to calculate Pearson's Coefficient for Figure 6 because JACoP does not have ROI selection capabilities. The Fpn-GFP channel was set to Ch1 and the mCherry-TfnR channel was set to Ch2, an ROI was selected in the GFP channel encircling the cytoplasm and excluding the plasma membrane of the cell. Pearson's Coefficient was calculated using 1 slice per cell.

2.10 Statistical analysis

GraphPad Prism 7 software was used to perform statistical tests and generate graphs (GraphPad software, La Jolla, CA). Data was analyzed statistically using unpaired t-tests or two-way analysis of variance with either Tukey's or Dunnet's multiple comparisons test as indicated. Significance was set to $p < 0.05$.

CHAPTER 3 – RESULTS

3.1 Fpn is removed from phagosomes harbouring *S. aureus* or IgG-coated beads

Trafficking of Fpn during phagocytosis is not characterized and to rectify this I sought to determine if Fpn remains on the phagosome or if the protein is removed from the phagosome during maturation. To visualize Fpn trafficking within the phagocyte, I constructed a Fpn-GFP fusion protein as described in Chapter 2 and established that the Fpn-GFP fusion protein localizes to the plasma membrane as expected and does not perturb phagocytosis in RAW cells (see Appendix 1).

RAW cells expressing Fpn-GFP were i) exposed to IgG-coated beads (Fig 3A, top row) or ii) infected with *S. aureus* USA300 carrying plasmid pAH9 (pAH9 expresses mCherry; see Table 1) (Fig 3A, bottom row) and fixed 5, 15, and 60 min post-addition of the phagocytic targets. All images were obtained using wide-field fluorescence microscopy and subsequently deconvolved unless otherwise indicated. The presence of Fpn-GFP on phagosomes containing staphylococci or IgG-coated beads was analyzed using the criteria outlined in section 2.9. Beads and bacteria that were not phagocytosed were labelled using a secondary antibody (magenta). Image analysis revealed that Fpn-GFP was depleted from maturing phagosomes irrespective of phagocytic target and that by 60 min approximately 90% of phagosomes were Fpn-negative (Fig 3C). Interestingly, I failed to detect uptake of *S. aureus* 5 min post-infection, demonstrating important differences in the phagocytic efficiency of RAW macrophages when ingesting targets through Fc γ receptors as opposed to other non-opsonic receptors (134).

To confirm the finding that Fpn is absent from late-stage phagosomes, using laser-scanning confocal microscopy I compared Fpn-GFP localization to that of LAMP1, a biochemical marker of late phagosomes and phagolysosomes (149), at 60 min post-phagocytosis. RAW cells expressing Fpn-GFP were exposed to IgG-coated beads (Fig 3B, top panel) or infected with eFluor670-labelled *S. aureus* USA300 (Fig 3B, bottom panel) and 1 hr after addition of targets, the cells were immunostained for LAMP1. Quantitation of the percentage of phagosomes showing LAMP1 accumulation revealed

that 75% or more of LAMP1-positive phagosomes are devoid of Fpn irrespective of the phagosomal cargo (Fig 3D).

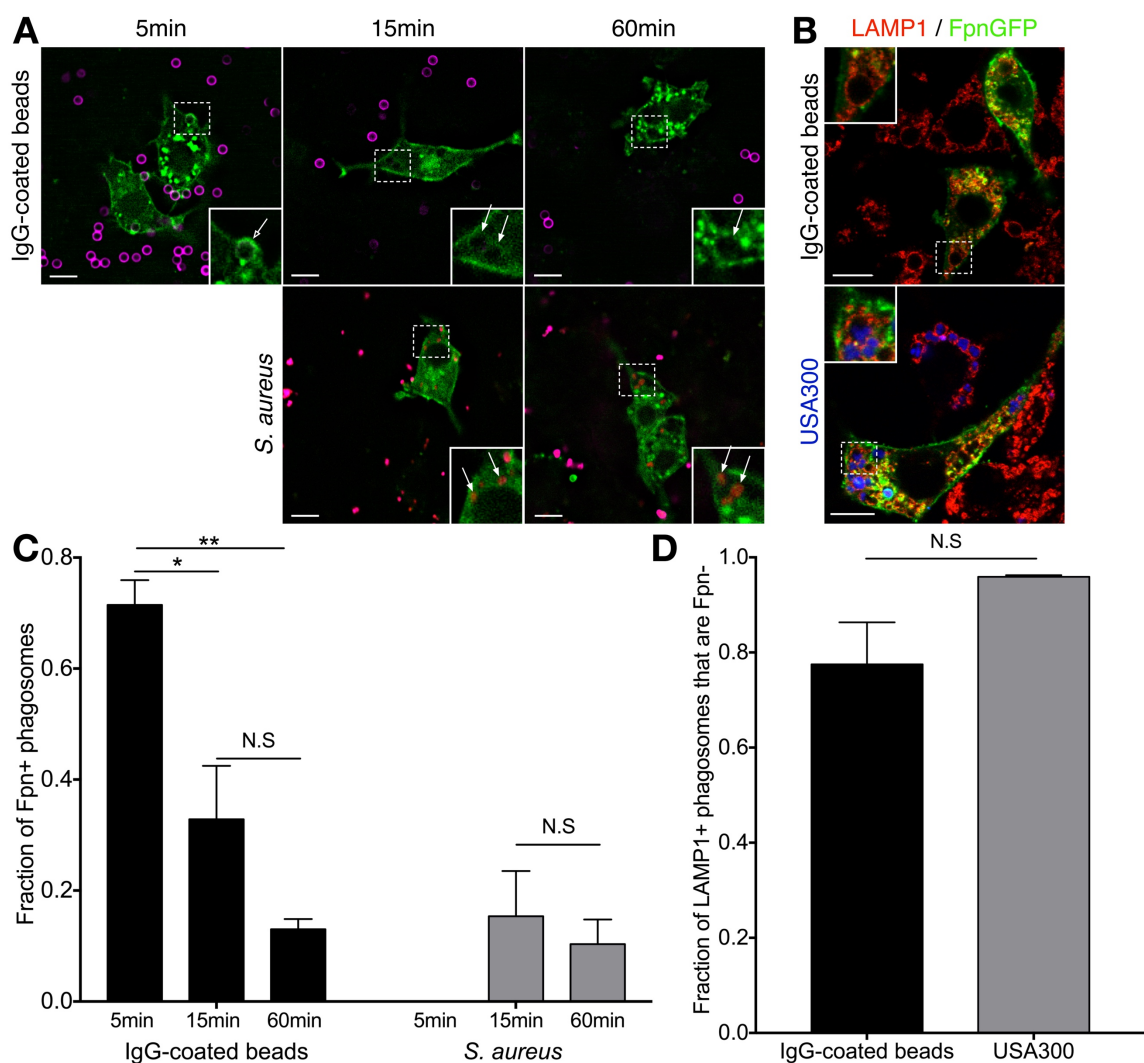


Figure 3. Fpn is depleted from the phagosome as it matures. (A) RAW macrophages expressing Fpn-GFP (green) were exposed to either IgG-coated beads (top row) or *S. aureus* pAH9 (red; bottom row) and fixed 5, 15, and 60 min post-addition of phagocytic targets. Extracellular beads and bacteria at each time point were fluorescently labelled (magenta). *S. aureus* was inefficiently phagocytosed at 5 min despite numerous cocci bound to phagocyte surfaces (not shown). A hollow arrow denotes a Fpn-positive phagosome and filled arrows indicate Fpn-negative phagosomes. Bar equals 10µm. (B) Confocal sections of RAW cells expressing Fpn-GFP exposed to either IgG-coated beads (top panel) or infected with eFluor670-labelled USA300 (bottom panel). Fluorescence micrographs depict the distribution of endogenous LAMP1 (red) 1 hr after the addition of

phagocytic targets. White arrowhead points to a bead-containing phagosome. Bar equals 10 μ m. **(C)** Quantification of the fraction of Fpn-positive phagosomes at the indicated time points is presented. Data are the mean \pm SEM from ≥ 92 phagosomes from at least 3 independent experiments. Statistical significance was determined using two-way ANOVA with Tukey's multiple comparisons test, where * $p < 0.05$, ** $p < 0.01$, and n.s is not significant. **(D)** Quantification of the fraction of phagosomes that are LAMP1-positive and Fpn-negative. The graph represents the mean \pm SEM from ≥ 129 LAMP1-positive phagosomes derived from 3 independent experiments. Statistical significance was determined using an unpaired t-test, where n.s is not significant.

3.2 Selective exclusion of Fpn from LAMP1-positive phagosomes

While comparing Fpn-GFP and LAMP1 localization in USA300-infected RAW cells, I observed that non-phagosomal, discrete GFP-positive puncta were localized throughout the cytosol of Fpn-GFP expressing cells, and that these puncta co-localized with LAMP1. Interestingly, phagocytosed cocci resided in LAMP1-positive but Fpn-GFP-negative phagosomes at this same time point. Implicit in this observation is that not all LAMP1 positive compartments are created equally and that there is a mechanism to selectively exclude Fpn from LAMP1 containing phagosomes while directing Fpn to other LAMP1 positive compartments that are not phagosomes (Fig 4).

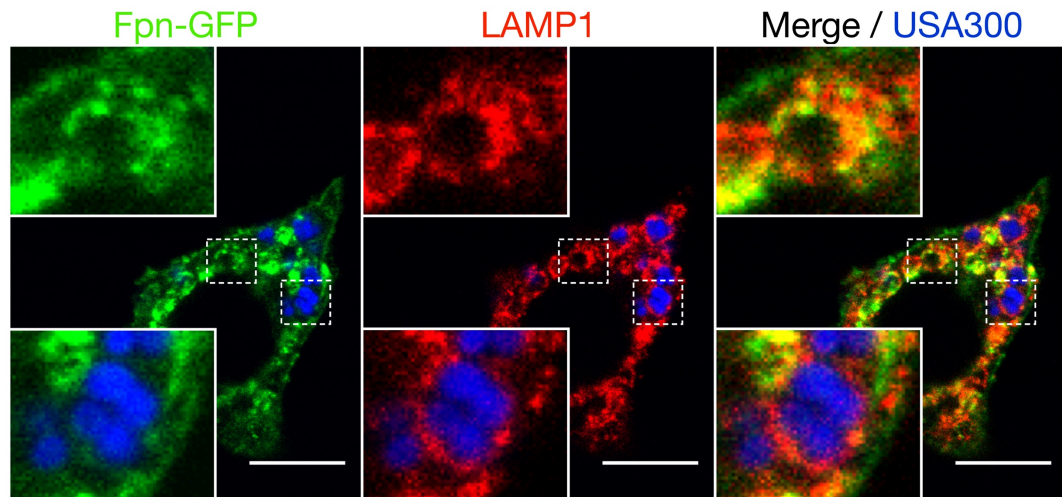


Figure 4. Selective exclusion of Fpn from LAMP1-positive phagosomes. Confocal sections depicting the distribution of endogenous LAMP1 (red) in RAW cells expressing Fpn-GFP (green) is shown. RAW macrophages were incubated with eFluor670-labelled *S. aureus* USA300 for 60 min and then immunostained. The insets depict the absence of GFP from LAMP1-positive phagosomes (bottom) and co-localization of Fpn-GFP puncta with LAMP1 (top). Bar equals 10 μ m.

3.3 Inhibition of acidification does not prevent Fpn removal from the phagosome

As Fpn is present on some early phagosomes (Fig 3A, hollow arrow), I concluded that Fpn exclusion from the phagosome is unlikely (Fig 2F). Multivesicular body formation and phagosome-lysosome fusion occur in the late stages of phagosome maturation and because Fpn is removed early in the phagosome maturation process, I postulated that it is unlikely that Fpn removal is occurring via these late-stage processes. Degradation of phagocytic cargo in these processes is, in part, mediated by the acidification of the phagosome and so I sought to test this postulation by inhibiting acidification using the vATPase inhibitor Concanamycin A (CcA) (176). RAW cells were pre-treated with a vehicle control (DMSO) or 500 nM CcA for 30 min in SF-RPMI. To confirm inhibition of acidification, after 30 min treatment, cells were stained with the acidotropic probe LysoTracker® Red DND-99 and imaged live using identical acquisition parameters for each condition (Fig 5A). In vehicle control treated cells, regions of LysoTracker® accumulation were present indicating acidic vacuoles. In comparison, in cells treated with CcA, LysoTracker® accumulation was completely ablated demonstrating the absence of acidic vacuoles and the efficacy of CcA treatment. After confirming CcA treatment was working, to test if acidification mediated Fpn removal, RAW cells expressing Fpn-GFP were pre-treated with vehicle control or 500 nM CcA for 30 min in SF-RPMI. At this point, IgG-coated beads were added, cells were maintained in the presence of 500 nM CcA, and allowed to phagocytose for 30 min before fixation (Fig 5B). Quantification revealed that there was no significant difference in the fraction of Fpn-positive phagosomes in CcA treated cells compared to control (Fig 5C). This finding supports the postulation that Fpn removal from the phagosome likely occurs through a mechanism other than MVB-mediated or lysosomal degradation.

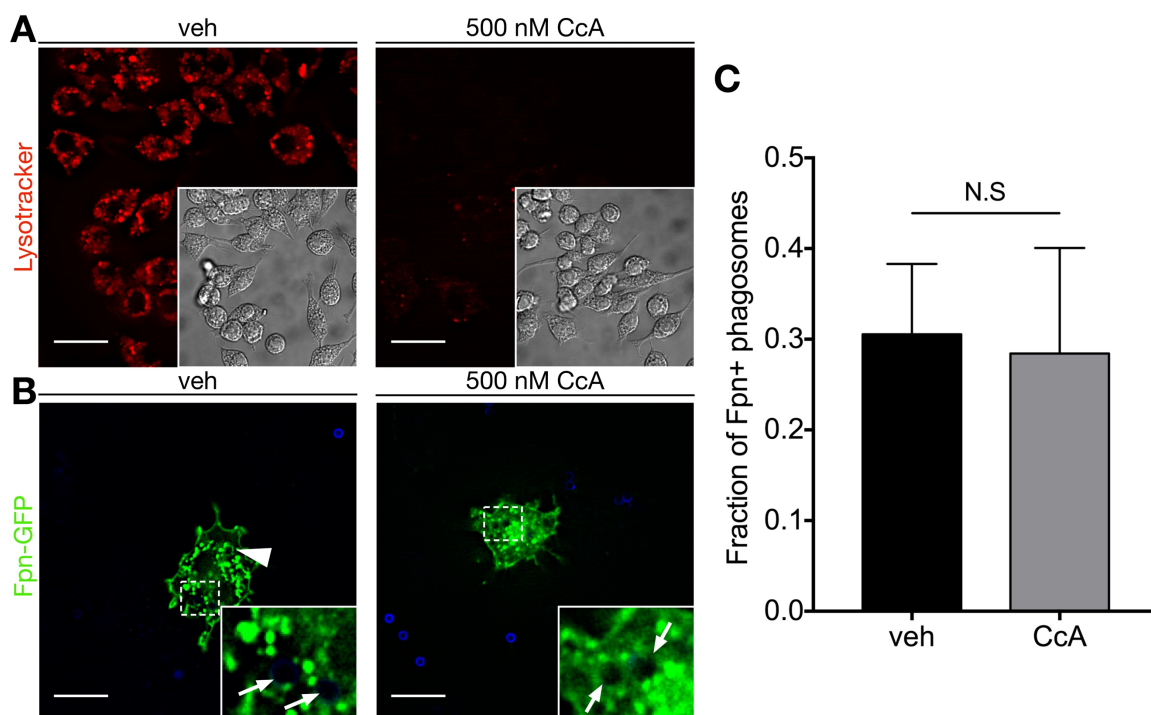


Figure 5. Phagosomal loss of Fpn is not altered upon inhibition of acidification. (A) RAW macrophages pre-treated with a vehicle control (veh) or 500 nM CcA for 30 min were exposed to 250 nM LysoTracker® Red for 10 min, washed, and imaged live. Images were taken using identical acquisition parameters between conditions. Insets depict corresponding differential interference contrast images. Bar equals 20 μ m. **(B)** RAW cells expressing Fpn-GFP were treated as above except after 30 min pre-treatment, IgG-coated beads were added and cells allowed to phagocytose for 30 min. Arrows in insets indicate Fpn-negative phagosomes while the arrowhead indicates a Fpn-positive phagosome. Extracellular beads were labelled fluorescently (blue). Bar equals 20 μ m. **(C)** Quantification of the fraction of Fpn-positive phagosomes for the indicated treatment. Data are the mean \pm SEM from ≥ 95 phagosomes from at least 3 independent experiments. Statistical significance was determined using an unpaired t-test, where n.s is not significant.

3.4 Fpn and TfnR do not co-localize in the cytoplasm of macrophages

Since Fpn removal from the phagosome occurs early during phagosome maturation (Fig 3C) I next sought to investigate whether Fpn is removed and recycled back to the plasma membrane.

To investigate this possibility, I compared the distribution of Fpn throughout the cell to that of TfnR - a prototypical marker of the recycling pathway (172). RAW macrophages were co-transfected with plasmids encoding Fpn-GFP and mCherry-TfnR, IgG-coated beads were added to initiate phagocytosis, and the cells were fixed 15 min after addition (Fig 6A). Outside beads were labelled using a secondary antibody (blue). Image analysis software was used to calculate the degree of co-localization between Fpn and TfnR. If the proteins use the same trafficking mechanism, overlap between the two signals should occur. However, calculating Pearson's coefficient on the entire cell would likely indicate some degree of co-localization since both Fpn and TfnR localize to the plasma membrane. To overcome this confounding factor, a region of interest (ROI) was drawn around the entire cytoplasm of the cell, excluding only the plasma membrane, and Pearson's coefficient was calculated using this ROI. Pearson's co-localization coefficient is a value that ranges from -1 to +1, where -1 is perfect negative-correlation, 0 is no correlation, and +1 is perfect correlation (177–179). The extreme values of Pearson's coefficient are easy to interpret while intermediate values are less conclusive. Knowing this, based on the ROI selected to exclude the plasma membrane from calculations, Fpn and TfnR did not demonstrate a high degree of co-localization on membranes inside of the macrophage (i.e. membranes other than the plasma membrane) (Fig 6B). These data indicate that Fpn and TfnR may use different trafficking mechanisms.

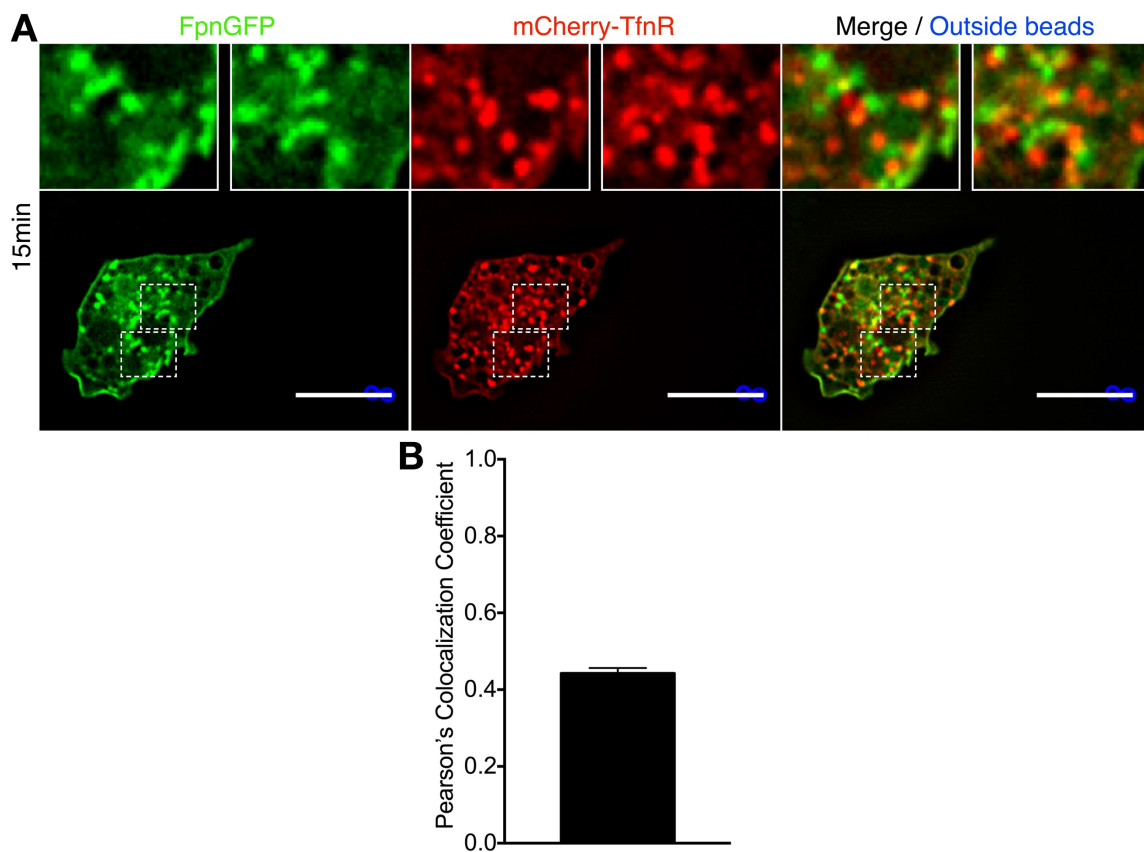


Figure 6. Fpn and TfnR do not co-localize in the cytoplasm of macrophages. (A) RAW macrophages co-expressing Fpn-GFP (green) and mCherry-TfnR (red) were exposed to IgG-coated beads and fixed 15 min post-addition of beads. Extracellular beads were labelled fluorescently (blue). Insets demonstrate regions within the cell where little overlap between signals occurs. Bar equals 20 μ m. **(B)** Graph depicts Pearson's colocalization coefficient from an ROI containing only the cytoplasm of each cell. Data are the mean \pm SD from 23 cells from 3 independent experiments.

3.5 TfnR co-localizes with Rab4 while Fpn does not

To further investigate the possibility that Fpn is recycled I wanted to determine if Rab4 is involved in Fpn removal from the phagosome. Rab4 is a GTPase that localizes to early endosomes and is involved in the fast recycling pathway (166, 180). The fast recycling pathway recycles cargo like TfnR from the early endosome back to the plasma membrane, bypassing the endocytic recycling compartment (162). RAW cells were co-transfected with plasmids encoding either GFP-Rab4 and mCherry-TfnR (Fig 7A) or GFP-Rab4 and Fpn-mRuby (Fig 7B), exposed to IgG-coated beads and fixed 15 min after initiation of phagocytosis. Beads were added to initiate the phagocytic process. Co-localization was measured using Mander's co-localization co-efficient. Mander's co-localization coefficient consists of two different values that both range from 0 to +1. They represent the fraction of pixels in one channel (ie. red channel) that have a corresponding pixel above a set threshold in a second channel (ie. green channel). The converse for the second coefficient is true (ie. the fraction of pixels in the green channel that have a corresponding pixel in the red channel) (177, 178). As mentioned above, Rab4 mediates the recycling of TfnR and thus I expected to observe co-localization between Rab4 and TfnR (Fig 7C). If Fpn trafficking is mediated by Rab4 I would expect a similar degree of co-localization between Rab4 and Fpn. However, Mander's coefficient for Fpn and Rab4 is significantly lower than that for TfnR and Rab4 (Fig 7C). This evidence suggests that Rab4 is not involved in the trafficking of Fpn and supports previous evidence (Fig 6) that Fpn is trafficked via a different mechanism than TfnR.

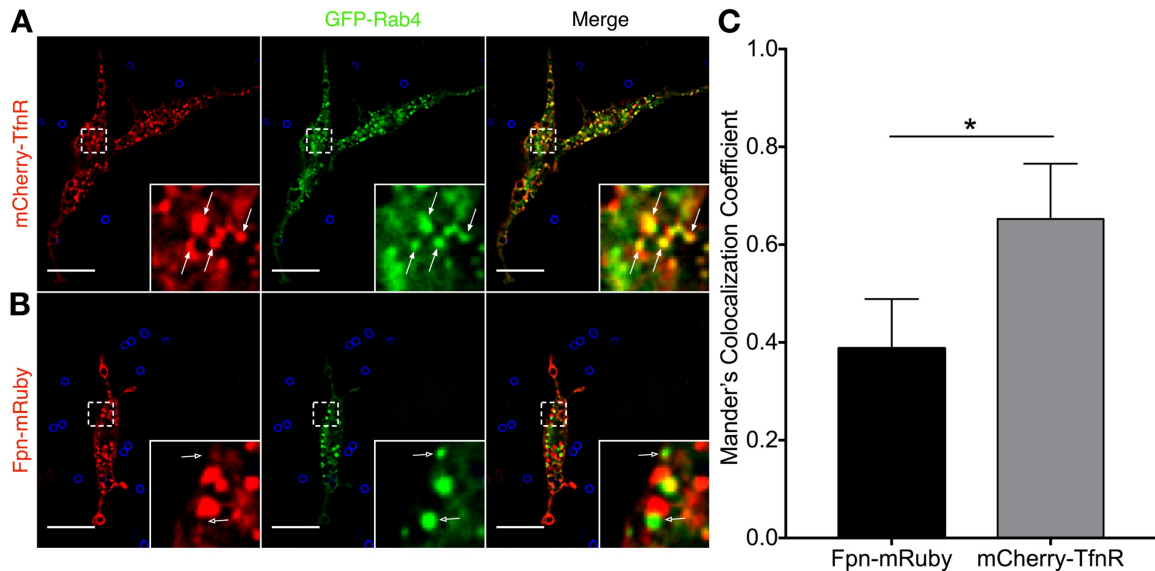


Figure 7. TfnR, but not Fpn, co-localizes with Rab4. (A) RAW macrophages expressing mCherry-TfnR (red) and GFP-Rab4 (green) were exposed to IgG-coated beads and fixed 15 min post-addition of phagocytic targets. Extracellular beads were labelled fluorescently (blue). Filled arrows denote Rab4 features that co-localize with TfnR puncta. Bar equals 20 μ m. (B) RAW cells expressing Fpn-mRuby (red) and GFP-Rab4 (green) were exposed to IgG-coated beads and fixed 15 min after addition of beads. Extracellular beads were labelled fluorescently (blue). Hollow arrows denote Rab4 features that do not co-localize with Fpn puncta. Bar equals 20 μ m. (C) Graph depicts Mander's coefficient for co-localization of GFP-Rab4 with either Fpn-mRuby or mCherry-TfnR. Data are the mean \pm SEM from ≥ 17 cells from at least 4 independent experiments. Statistical significance was determined using an unpaired t-test, where * $p < 0.05$.

3.6 Early PI(3)P-positive phagosomes show more Fpn depletion than TfnR depletion

Thus far, I have demonstrated that Fpn is removed from the phagosome via a mechanism that likely differs from the mechanism by which TfnR is removed from phagosomes. Based on this I wanted to further elucidate the kinetics of Fpn removal from the phagosome using different markers of the phagosome maturation process. RAW cells were transfected with plasmids encoding 2xFYVE-RFP and either Fpn-GFP or TfnR-GFP. 2xFYVE is a lipid biosensor of PI(3)P, a marker of early phagosomes (Fig 1) (147). The transfected cells were then exposed to IgG-opsonized beads and fixed 10 min post-initiation of phagocytosis (Fig. 8A). Early phagosomes, as indicated by the presence of 2xFYVE, were found to be largely (>95%) Fpn-negative (Fig 8B). In contrast, significantly more PI(3)P-positive, early phagosomes were TfnR-positive (70%) ($p < 0.01$) (Fig 8B). This marked difference in the phagosomal distribution of Fpn and TfnR again indicates that Fpn is removed from the phagosome through a different mechanism than TfnR.

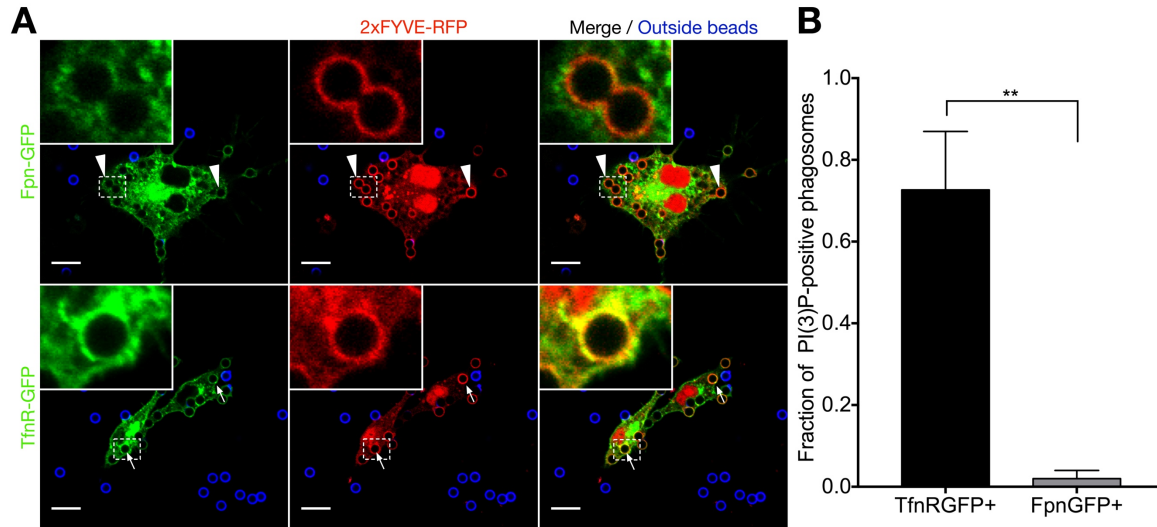


Figure 8. Early PI(3)P positive phagosomes show more Fpn depletion than TfnR depletion. (A) Confocal sections depicting RAW macrophages expressing Fpn-GFP (top row) or TfnR-GFP (bottom row) (green) and the PI(3)P biosensor 2xFYVE-RFP (red) that were allowed to phagocytose IgG-coated beads for 10 min. After fixation, the presence of phagosomal Fpn-GFP, TfnR-GFP, and 2xFYVE-RFP was analyzed. Arrows indicate a TfnR and 2xFYVE-positive phagosome while arrowheads indicate a Fpn-negative but 2xFYVE-positive phagosome. Bar equals 10 μ m. (B) The graph depicts the fraction of 2xFYVE-positive phagosomes that are positive for either Fpn- or TfnR-GFP. The data represents the mean \pm SD derived from \geq 56 phagosomes from at least 3 independent experiments. Statistical significance was determined using an unpaired t-test, where ** $p < 0.01$.

3.7 The PI3K inhibitor LY294002 alters cellular distribution of TfnR but not Fpn

The accumulation of PI(3)P on the early phagosome is due to the acquisition of Vps34, the Class III PI3K responsible for the catalysis of PI to PI(3)P (147). Based on this role of PI3K, I wanted to determine if Fpn trafficking throughout the cell is dependent upon PI3K. To do this I used the PI3K inhibitor LY294002 (181). Observation of the distribution of either Fpn or TfnR throughout the cell revealed that while the distribution of TfnR was altered upon exposure to LY294002 (Fig 9A) the distribution of Fpn was unaffected (Fig 9B). More specifically, in vehicle control treated cells TfnR was found largely at the plasma membrane (Fig 9A, arrowheads). As has been reported previously (172), upon treatment with 100 μ M LY294002 in TfnR-GFP expressing cells enlarged endosomal vesicles (Fig 9A, filled arrows) or a large perinuclear accumulation of TfnR (Fig 9A, hollow arrows) was observed thus demonstrating the efficacy of LY294002-treatment in altering protein trafficking. Interestingly, no observable change in distribution of Fpn occurred upon PI3K inhibition (Fig 9B). This finding provides evidence that LY294002 treatment is functional, provides further evidence that Fpn and TfnR are trafficking through different mechanisms, and alludes that PI3K activity is not essential for Fpn trafficking.

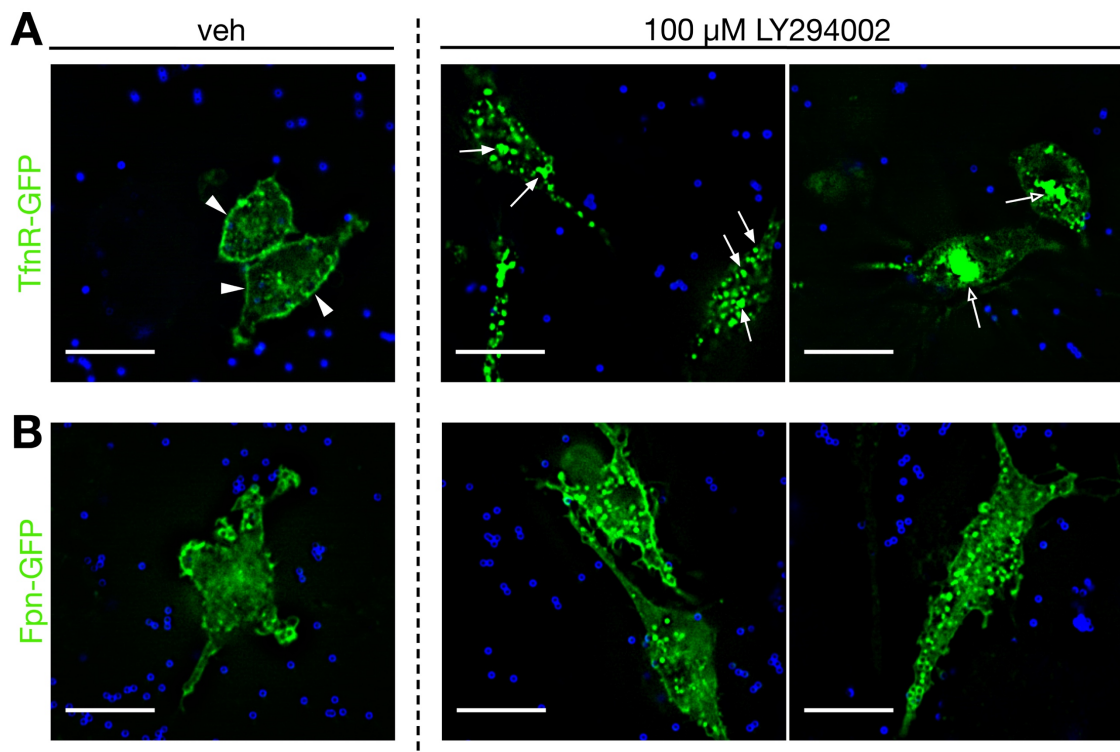


Figure 9. The cellular distribution of TfnR but not Fpn is altered upon exposure to a PI3K inhibitor. RAW cells transfected with either (A) TfnR-GFP or (B) Fpn-GFP were pre-treated with 100 μ M LY294002 or with a vehicle control (veh) for 30 min. IgG-coated beads were then added to initiate phagocytosis and cells were fixed 30 min after addition. Extracellular beads were labelled fluorescently (blue). Bar equals 20 μ m. In (A), arrowheads highlight the presence of TfnR primarily at the plasma membrane in vehicle control treated cells. Filled arrows emphasize enlarged TfnR-containing endosomal vesicles and hollow arrows indicate the perinuclear accumulation of TfnR in LY294002-treated cells.

3.8 PI3K-independent removal of Fpn from the phagosome

Based on the findings that Fpn is removed from the phagosome before PI(3)P accumulates (Fig 8) and that Fpn trafficking is not altered upon PI3K inhibition I next wanted to look expressly at phagosomal populations of Fpn. More specifically, I wanted to determine if Fpn removal from the phagosome is dependent upon the activity of PI3K, which precedes PI(3)P accumulation on the phagosome. To do this, I again used the PI3K inhibitor LY294002 (181). I expected that if Fpn removal is dependent on PI3K, upon PI3K inhibition Fpn removal from the phagosomal membrane would be delayed. RAW cells transfected with Fpn-GFP and 2xFYVE-RFP were pre-treated with 100 μ M LY294002 for 10 min before addition of IgG-coated beads. Beads of 1.5 μ m in size were used because PI3K inhibition has been shown to only hinder phagocytosis of large targets (>5 μ m) (182). Interestingly comparison of the fraction of Fpn-positive phagosomes in treated versus untreated macrophages yielded no difference between both conditions (Fig 10). The absence of 2xFYVE-RFP-positive phagosomes in LY294002 treated cells versus vehicle control indicates that the LY294002 treatment was effective and blocked PI(3)P accumulation on the phagosome. This finding indicates that Fpn removal from the phagosome occurs independently of PI3K activity. Moreover, as MVB formation is PI(3)P-dependent (183) and inhibition of Vps34 does not alter Fpn removal, it stands to reason that MVB formation is not a major contributor to loss of Fpn from the phagosomal membrane.

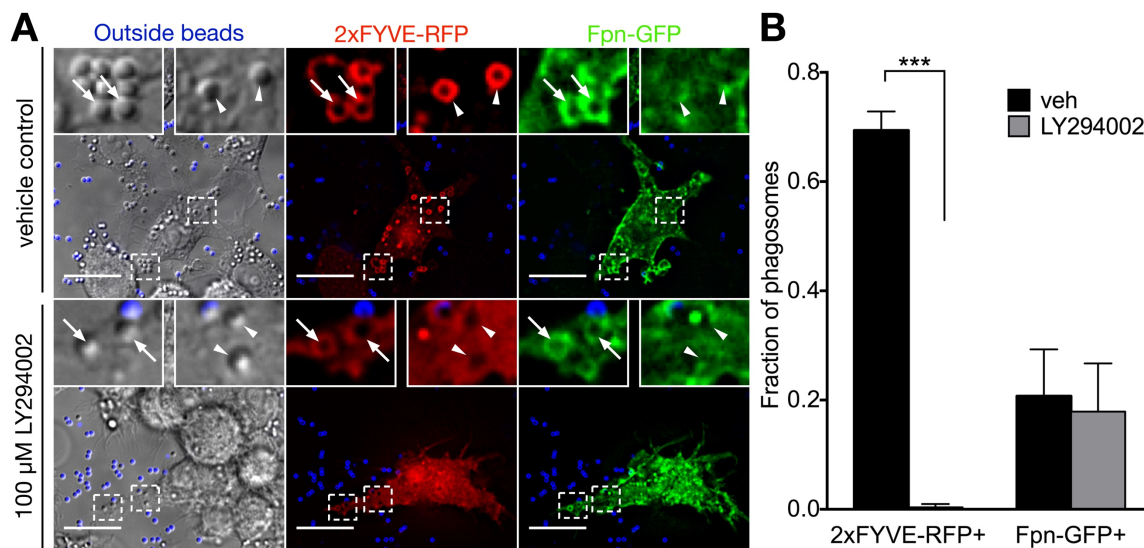


Figure 10. Fpn removal from the phagosome occurs independently of PI3K. (A) RAW cells expressing the PI(3)P-biosensor 2xFYVE-RFP (red) and Fpn-GFP (green) were pre-treated with DMSO (vehicle control) or 100 μ M LY294002 (PI3K inhibitor) for 10 min. IgG-coated beads were added for 10 min before fixing and the fraction of 2xFYVE-RFP- and Fpn-GFP-positive phagosomes were quantified. Beads that were not phagocytosed are labelled in blue. Arrowheads indicate Fpn-negative phagosomes while arrows indicate Fpn-positive phagosomes. Bar equals 20 μ m. **(B)** Graph depicts the fraction of phagosomes positive for 2xFYVE-RFP or Fpn-GFP from either vehicle control or LY294002 treated cells. The data represent the mean \pm SEM from \geq 100 phagosomes from 3 independent experiments. Statistical significance was determined using unpaired t-tests, where *** $p < 0.001$.

3.9 Fpn co-localizes with Rab5 during the early stages of phagosome maturation

Because Fpn removal from the phagosome membrane occurs independently of PI3K (Fig 10), I next investigated earlier events in the phagosomal maturation process by observing Rab5. Rab5 is a GTPase that is recruited to the nascent phagosome and is necessary for the recruitment of the PI3K Vps34 (184). RAW cells were co-transfected with plasmids encoding Fpn-GFP and Rab5WT-mCherry, exposed to IgG-coated beads and fixed 5, 9, and 15 min after initiation of phagocytosis (Fig 11A). Quantification revealed that approximately 75% of Rab5-containing phagosomes also contained Fpn at all three time points (Fig 11B). In addition, co-localization was observed between non-phagosomal Fpn-GFP puncta and Rab5WT-mCherry features in many cells (Fig 11A, arrowheads). This observation was confirmed using Pearson's coefficient which indicates that indeed these fluorescent proteins partially co-localize (Fig 11C). Due to the partial co-localization, it is conceivable that Rab5 could influence Fpn trafficking.

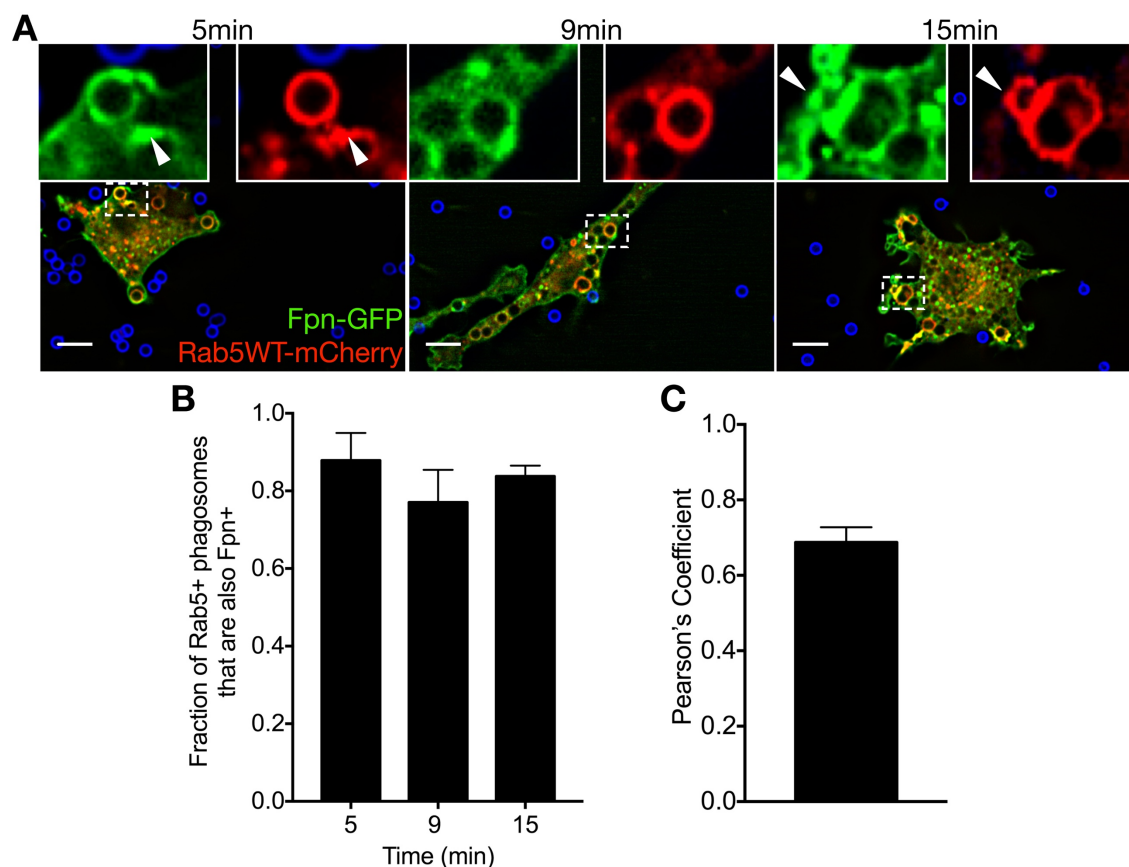


Figure 11. Fpn co-localizes with Rab5 during the early stages of phagosome maturation. (A) RAW cells were co-transfected with plasmids encoding Rab5WT-mCherry (red) and Fpn-GFP (green) and fixed 5, 9, and 15 min after addition of IgG-coated beads. Outside beads were labelled fluorescently (blue). Insets highlight Rab5-positive and Fpn-positive phagosomes. Arrowheads indicate non-phagosomal Rab5 features that are also Fpn-positive. Bar equals 10 μ m. (B) Graph depicts the fraction of Rab5-positive phagosomes that also contain Fpn at the indicated time point. Data are the mean \pm SD from ≥ 32 cells, ≥ 47 Rab5-positive phagosomes from 3 independent experiments. (C) Graph depicts Pearson's co-localization coefficient for Rab5WT-mCherry- and Fpn-GFP-expressing cells. Data are the mean \pm SD from 17 cells from 2 independent experiments.

3.10 Fpn removal is temporarily delayed in cells expressing constitutively active Rab5

Due to the co-localization between Fpn and Rab5, I next sought to determine whether Rab5 plays a functional role in the removal of Fpn from the phagosome. To do this, RAW cells were co-transfected with plasmids encoding Fpn-GFP and either Rab5WT-mCherry (Fig 12B), Rab5CA-mCherry (Fig 12C), or a soluble mCherry protein as a negative control (Fig 12A). Constitutively active (CA) Rab proteins are mutants that are locked in the GTP-bound, active state. Soluble mCherry (p-mCherryN1) was used as a control to demonstrate that expression of CA Rab5 and not mCherry alone alters Fpn trafficking. IgG-coated beads were added and the cells were fixed 9, 15, 30, 45, and 60 min after addition. The fraction of Fpn-positive phagosomes within each co-transfected cell was quantified (Fig 12D). At 9 min, all three states had similar proportions of Fpn-positive phagosomes. However, at both 15 and 30 min there was significant increase in the fraction of Fpn-positive phagosomes in CA Rab5 expressing cells compared to the soluble mCherry control ($p < 0.05$) but this difference was lost by 45 min. This may be because the endogenously active Rab5 can overcome the effects of the transfected CA Rab5. These data, combined with the Rab5/Fpn co-localization data (Fig 11), suggest that Rab5 could play a functional role in the removal of Fpn from the phagosome.

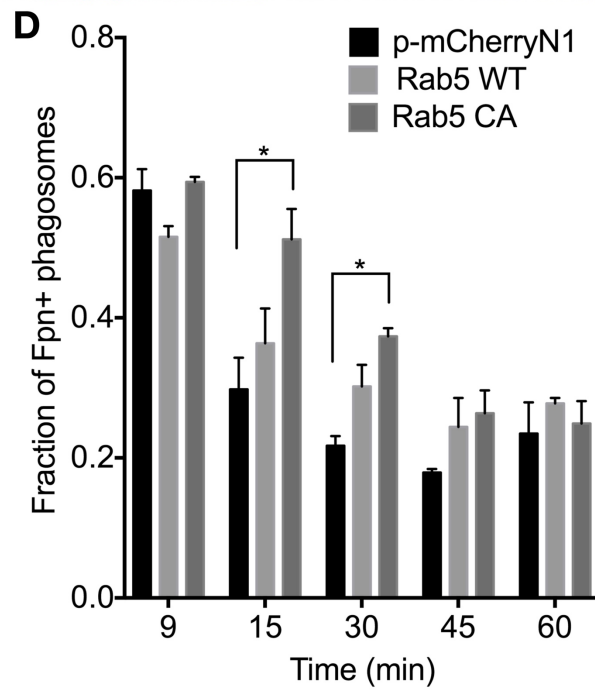
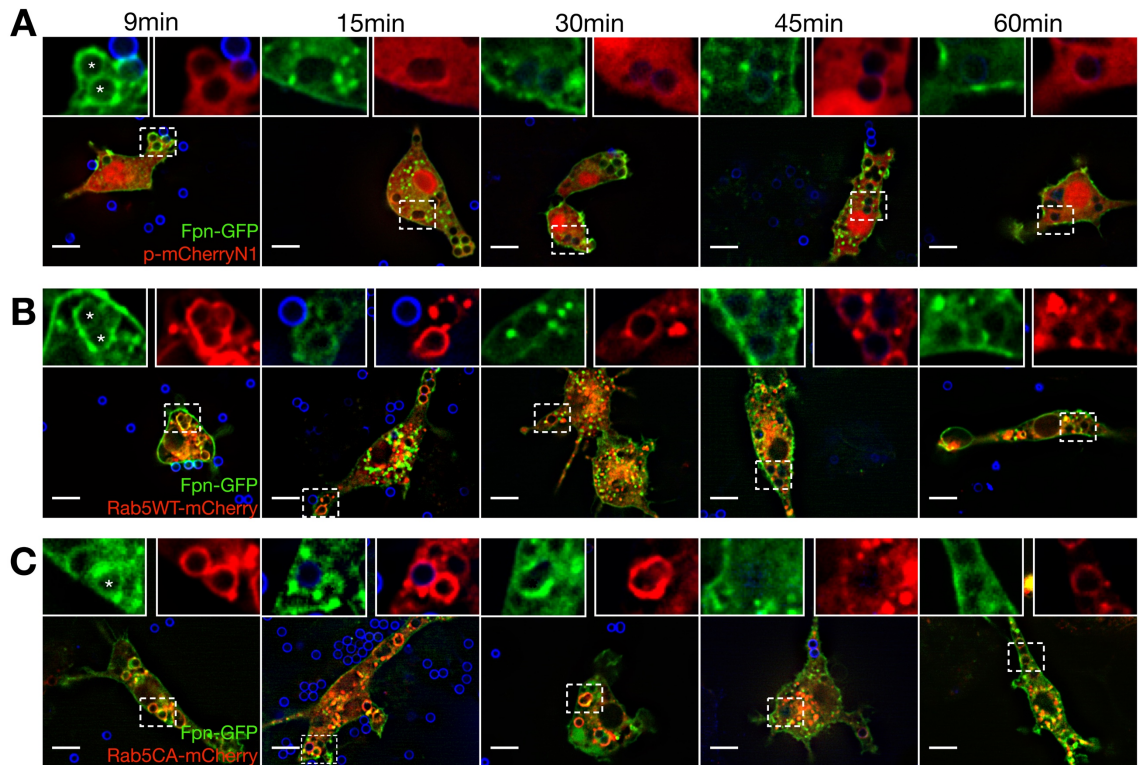


Figure 12. Fpn removal is temporarily delayed in cells expressing a constitutively active Rab5. (A) RAW cells were co-transfected with plasmids encoding soluble mCherry (p-mCherryN1; red) and Fpn-GFP (green) and were fixed 9, 15, 30, 45, and 60 min after addition of IgG-coated beads. Outside beads were labelled fluorescently (blue). Asterisks (*) highlight Fpn-positive phagosomes. (B) Same as (A) but cells were co-transfected with Rab5WT-mCherry (red) and Fpn-GFP (green). (C) Same as (A) but cells were co-transfected with Rab5CA-mCherry (red) and Fpn-GFP (green). (D) Graph depicts fraction of Fpn-positive phagosomes in cells co-transfected with the indicated plasmids. Data are the mean \pm SEM from ≥ 17 cells, ≥ 88 phagosomes from at least 2 independent experiments. Statistical significance was determined relative to control cells expressing p-mCherryN1 using two-way ANOVA with Dunnet's multiple comparisons test, where $*p < 0.05$. Bar equals 10 μ m.

3.11 Fpn is present on some Rab7-containing phagosomes

I next analyzed Rab7-mCherry expressing cells for the presence of Fpn-positive phagosomes. Rab7 is a GTPase that is recruited to the phagosome after Rab5 accumulation and is a marker of late stage phagosomes (148) (Fig 1). This comparison was performed to demonstrate that it is specifically the over-expression of Rab5 and not simply the over-expression of any Rab protein that is causing the temporary retention of Fpn on the phagosome. To do this, RAW cells expressing Fpn-GFP and Rab7-mCherry were exposed to IgG-coated beads and fixed 15, 30, 45, and 60 min post-addition of phagocytic targets (Fig 13A). I then quantified the fraction of Fpn-positive phagosomes in Rab7-mCherry expressing cells, regardless of Rab7 presence on the phagosome (Fig 13C). This analysis revealed no difference in the fraction of Fpn-positive phagosomes between Rab7 and soluble mCherry expressing cells providing further evidence that Fpn retention on the phagosome is a Rab5-specific event.

While performing this analysis, I also wanted to determine the degree of Fpn and Rab7 co-localization on the phagosome. Image analysis revealed that about 30% of phagosomes positive for Rab7 also contained Fpn (Fig 13B). This finding is surprising as analysis of early phagosomes demarcated by PI(3)P found that the majority of PI(3)P-positive phagosomes were Fpn-negative (Fig 8).

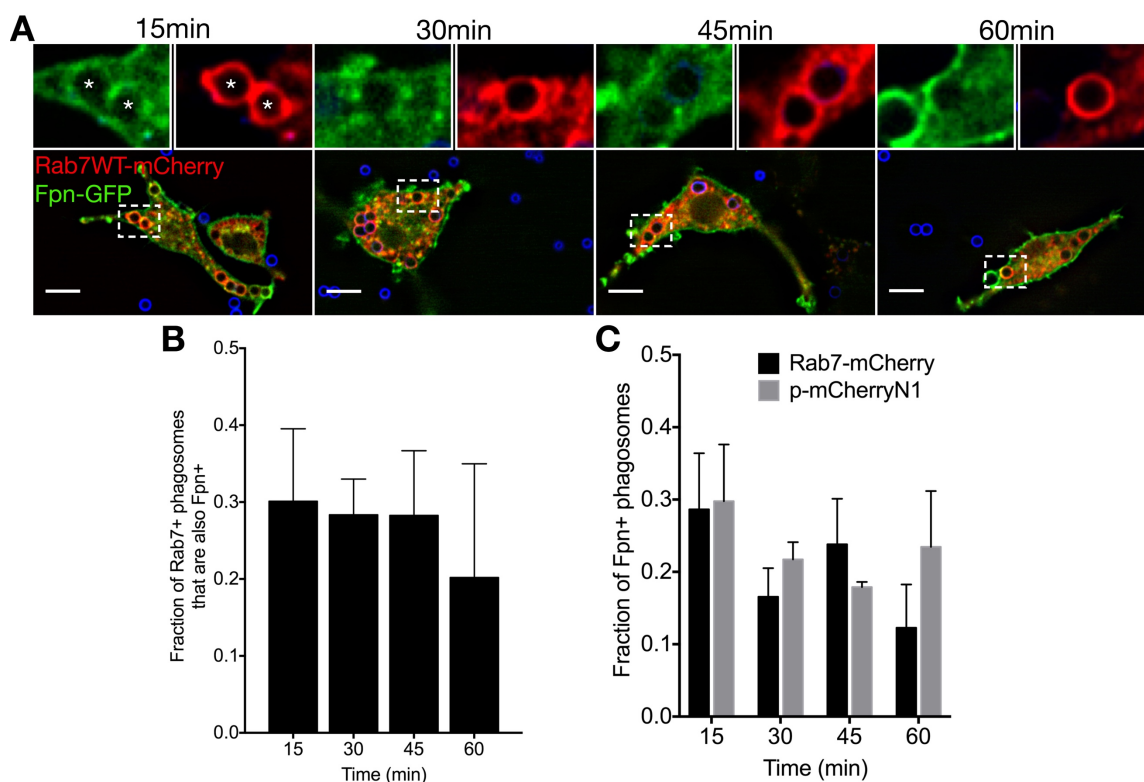


Figure 13. Fpn is present on some Rab7-containing phagosomes. (A) RAW cells were co-transfected with plasmids encoding Rab7-mCherry (red) and Fpn-GFP (green) and were fixed 15, 30, 45, and 60 min after addition of IgG-coated beads. Outside beads were labelled fluorescently (blue). Insets highlight either Rab7-positive and Fpn-positive phagosomes (*) or Rab7-positive and Fpn-negative phagosomes. Bar equals 10 μ m. **(B)** Graph depicts the fraction of Rab7-positive phagosomes that also contain Fpn at the indicated time point. Data are the mean \pm SD from ≥ 20 cells, ≥ 100 Rab7-positive phagosomes from 3 independent experiments. **(C)** Graph depicts fraction of Fpn-positive phagosomes in cells transfected with either p-mCherryN1 or Rab7-mCherry. Data are the mean \pm SD from ≥ 17 cells, ≥ 70 phagosomes from at least 2 independent experiments.

CHAPTER 4 – DISCUSSION and FUTURE DIRECTIONS

Iron is an essential nutrient required by virtually all forms of life and its acquisition and sequestration are important aspects of bacterial pathogenesis and host innate immunity, respectively. Collectively, the various mechanisms used to sequester nutrients and restrict access of essential metals like iron to pathogens is termed nutritional immunity (4). Host cells have both iron scavenging proteins and iron transporting proteins that together render iron inaccessible to invading microbes.

Because iron is an essential nutrient for the host it follows that maintaining iron at homeostatic levels is also critical. Pivotal to iron homeostasis, Fpn is an iron transporting protein found in the plasma membrane of macrophages that pumps iron from the cytoplasm to the extracellular environment of the macrophage. The function of Fpn is modulated by hepcidin, a hormone produced by the liver. In response to inflammation, iron overload, or infection, hepcidin is produced and binds directly to Fpn, resulting in its endocytosis and ultimately its degradation (38, 124, 185); the net effect of this process is to reduce the pool of extracellular, or ‘labile’, iron available to invading pathogens. In contrast, in bacterially infected cells an increase of Fpn mRNA is observed leading to increased expression of Fpn at the plasma membrane (129–131). The net effect of this occurrence is increased iron export from the cell thereby limiting iron access to intracellular pathogens (131, 186). However, in infected macrophages that have i) not been exposed to hepcidin or that have ii) increased Fpn expression at the membrane, it is possible that after phagosome formation Fpn may reside on the phagosomal membrane. This is because upon phagosome formation the composition of nascent phagosomes largely resembles the composition of bulk plasma membrane. So, due to the orientation of Fpn, Fpn residing on the phagosome would transport iron into the pathogen-containing phagosomal compartment, potentially aiding the replicative capacity of the ingested microbes (Fig 2B).

To this end, I sought to investigate what happens to Fpn in the early stages of infection before hepcidin production is increased using a model of phagocytosis in which Fpn is over-expressed at the membrane. This model presumably replicates the net effect of increased Fpn expression in response to infection. My findings suggest that Fpn is lost

from the phagosomal membrane during early stages of phagosome maturation thus supporting the hypothesis that the host removes Fpn from the phagosome to prevent phagocytosed bacteria from obtaining iron.

At the outset of this study, four mechanisms of Fpn removal from the phagosome were postulated. As shown in Figure 2, I proposed that: i) Fpn may be recycled back to the plasma membrane (Fig 2E), ii) it may be proteolytically degraded while residing in the phagosomal membrane (Fig 2D), iii) Fpn may be degraded in the lumen of the phagosome as part of a MVB (Fig 2C), or iv) Fpn may be excluded from the phagosomal membrane altogether (Fig 2F).

While the composition of nascent phagosomes generally resembles that of the plasma membrane, selective exclusion of certain membrane-associated proteins, like the tyrosine phosphatase CD45, from the phagosome has been described (187). Since Fpn-positive phagosomes were observed throughout the study, recall the large fraction of early Rab5-containing phagosomes that are also Fpn-positive (Fig 11), I concluded that Fpn is not excluded from the phagosome.

Despite the presence of Fpn on the early phagosome, I found that Fpn was ultimately eliminated from the phagosomal membrane. More specifically it was removed early during phagosome maturation and is gone by phagolysosomal formation for both phagosomes containing IgG-opsonized beads or *S. aureus* (Fig 3). This finding is in contrast with a previous finding that 2 h post-infection, phagosomes containing *M. tuberculosis* are Fpn-positive (132). This discrepancy may be attributed to the fact that *M. tuberculosis* perturbs phagosome maturation and the trafficking of endomembranes (157–159).

My findings demonstrate that inhibition of phagosomal acidification had no effect on Fpn removal from the phagosome (Fig 5) suggesting Fpn is not removed from the phagosome through a degradative mechanism. By pharmacologically inhibiting phagosomal acidification, phagosome maturation and all the degradative mediators therein – namely phagosome-lysosome fusion, delivery of lysosomal proteases, activation of proteases – are effectively halted (188, 189). A conceptually similar experiment utilized pharmacological agents to inhibit endosomal acidification to investigate EGFR degradation, the prototypical protein degraded via MVB formation. In this case,

inhibition of the vATPase using Bafilomycin A (functionally similar to CcA) prevented EGFR degradation (190). Notably, this study was investigating endosomal EGFR and not phagosomal EGFR specifically. So, while it provides precedence for using pharmacological agents to investigate protein degradation, it is important to note that endosomes and phagosomes are distinct organelles and differences are not uncommon. Nevertheless, the finding that inhibition of phagosomal acidification did not result in Fpn retention on the phagosome suggests that removal of Fpn from the phagosome does not occur through lysosomal-mediated degradation.

Further evidence to support the notion that Fpn removal from the phagosome does not occur through lysosomal-mediated degradation is that Fpn is lost from the phagosome during early stages of maturation when phagosomes are demarcated by PI(3)P (Fig 8). Therefore, it is unlikely that Fpn remains on the phagosomal membrane long enough for phago-lysosomal fusion to occur. The finding that late stage LAMP1-containing phagosomes do not contain Fpn further supports this presumption (Fig 3 BD). It should be noted that the absence of Fpn on mature LAMP1-positive phagosomes is not due to acidification-mediated quenching of GFP signal. The pTF1 plasmid used throughout this study encodes GFP fused to the C terminus of Fpn and both termini of Fpn are intracellular. This indicates that upon phagosome formation, both termini would remain cytosolic and the GFP fluorescence would not be sensitive to phagosomal acidification. Further, upon fixation, pH gradients across membranes are lost, therefore if the GFP signal was quenched in an acidic compartment, GFP would still be detected in fixed samples if the chromophore of the fluorescence protein is intact. Therefore, the absence of GFP signal on the LAMP1-positive phagosome is due to absence of Fpn and not merely a loss of GFP fluorescence.

At the outset of this study it was also proposed that Fpn may be removed from the phagosome by formation of a MVB. Some receptors in the phagosomal membrane get sorted into MVBs for subsequent degradation upon lysosome fusion (191). One example is the membrane receptor FcγRIIA which is ubiquitinated, sorted into a MVB, and then degraded (192). Formation of MVBs requires PI3K activity (193) to recruit Hrs, a PI(3)P effector protein important in sorting of ubiquitinated proteins (194). My data demonstrating that Fpn is removed from the phagosome even when PI3K is inhibited (Fig

10) suggests Fpn is not removed from the phagosome via MVB formation. If MVB formation was the mechanism of removal, I would expect to see Fpn retention on the phagosome during PI3K inhibition. Further, PI(3)P is required for sorting of proteins, such as EGFR, into MVBs (183). My data demonstrates that Fpn is absent from PI(3)P-containing phagosomes (Fig 8) indicating that Fpn has been removed before sorting of proteins into MVBs occurs. However, to more conclusively demonstrate that Fpn is not removed via MVB formation, I could generate a Fpn mutant that does not get ubiquitinated, as has been done previously (124). This mutant should still be found on the phagosome since phagosomes are derived from bulk membranes. However, since ubiquitination is required for sorting of proteins into MVBs, if the Fpn mutant is still removed from the phagosome, I would be able to conclude that Fpn removal is not mediated by MVB formation.

The finding that intracellular vesicles containing Fpn co-localize with LAMP1 throughout the cell (Fig 4) has previously been reported (38, 195). The novelty in this finding is that Fpn is selectively excluded from LAMP1-containing phagosomes. It is possible that in our system, the vesicles containing Fpn that co-localize with LAMP1 may have been internalized via hepcidin found in the serum-containing media and has been targeted for degradation. Therefore, it is conceivable that our system consists of two distinct internalized populations of Fpn: the hepcidin-mediated internalized fraction and the phagocytosis-mediated internalized fraction.

Overall, my findings also indicate that Fpn trafficking from the phagosome does not use the same mechanism as hepcidin-mediated internalization of Fpn. Recall, upon binding to hepcidin, Fpn is ubiquitinated (124), internalized and then trafficked through the MVB pathway (125) for lysosomal degradation (38). It is important to note that while phagocytosis and endocytosis share many common characteristics, notably endosomes and phagosomes undergo similar a maturation process, they represent distinct trafficking pathways within the cell and have many differences as well. For example, phagocytosis requires F-actin polymerization but does not require clathrin or dynamin, while endocytosis requires clathrin and dynamin but not actin polymerization (196). Another difference is that Fc γ RIIA-mediated endocytosis requires ubiquitination, however Fc γ RIIA-mediated phagocytosis does not (197, 198). Therefore, the differences between

the endocytic trafficking mechanism of Fpn and my data regarding phagocytic internalization of Fpn are likely attributable to the differences in internalization through endocytosis versus phagocytosis. Functionally, Fpn internalization due to hepcidin binding signals that the body is trying to prevent iron export from the cell (123). It follows that the result of hepcidin-mediated internalization is degradation of Fpn rather than recycling back to the plasma membrane as this would counter the effect of the initial internalization. Alternatively, in our model of phagocytosis, RAW cells are exposed to relatively constant levels of hepcidin which is assumed to be present in the serum the cells are maintained in. In phagocytosis, Fpn internalization was not a result of hepcidin signaling and so the cell may not need to degrade it. In fact, in concert with NO-facilitated cellular increases in Fpn transcription in infected cells (121), the cell may recycle internalized Fpn back to the plasma membrane, possibly to aid in clearance of the intracellular bacteria. However, further investigation into this possibility is required.

It is important to note that in images of late stage phagosomes (Fig 3, Fig 13), Fpn-positive phagosomes were present however infrequently. A possible explanation is that despite efforts to synchronize phagocytosis, we do not know when phagocytosis of a particular target began and thus certain phagosomes truly represent early stages of maturation at which point Fpn is still present. Two options exist to approach this problem. One option is to use live-cell imaging and follow the phagocytosis and phagosome maturation of individual targets. Alternatively, I could perform phagocytosis assays as described with one change in that I would add fluorophore-conjugated Abs at specific time points after addition of phagocytic targets and before fixation. By doing this, during imaging, if the phagocytic cargo is labeled with an antibody I will know that phagocytosis of that target began after the specified time point.

Thus far, my evidence rules out the possibility that Fpn is excluded from the phagosome altogether as postulated at the outset of this study. Additionally, I have provided evidence that the phagosomal population of Fpn is not removed through degradative mechanisms, namely phagosome-lysosome fusion and MVB formation. The final proposed mechanism is recycling of Fpn back to the plasma membrane. Yet, when I compared Fpn localization to that of TfR, a protein known to be retrieved to the plasma membrane (141), co-localization did not occur (Fig 6). I have also shown that unlike

TfnR, Fpn does not co-localize with the fast recycling mediator Rab4 (Fig 7) (141). It remains possible that Fpn is recycled through mechanisms other than those already investigated as the cell utilizes many additional mechanisms of recycling that warrant investigation. For example, it is of interest to investigate the role of Arf6 in Fpn removal from the phagosome. Arf6 is a small GTPase that regulates protein trafficking within the cell and functions at the plasma membrane where it is involved in recycling (199). Arf6 has been shown to mediate the trafficking of many different proteins including: G-protein coupled receptors (200), MHC Class I (199), and β 1 integrin (201). As such, Arf6 is another plausible candidate to investigate as a mediator of Fpn trafficking. Additional protein recycling mechanisms that warrant investigation include SNX17 (202) and the WASH complex (203).

In addition to investigating the recycling mechanisms discussed above, future work aims to examine more closely the relationship between Rab5 and Fpn, specifically regarding the Rab5 effector protein APPL1. APPL1 (adaptor protein containing PH domain, PTB domains and leucine zipper) is an adaptor protein originally discovered for its role in Akt signaling (204) and has been shown to bind to and modulate the signaling of a number of transmembrane receptors (205–207). Because of the co-localization observed between Fpn and Rab5 (Fig 11), of interest to this project is the role of APPL1 as an effector protein of Rab5 (208). APPL1 is recruited to Rab5-containing phagosomes and, in cells expressing CA Rab5, APPL1 presence on the phagosome is prolonged (209). Further, it has been demonstrated that as PI(3)P accumulates on the phagosome, APPL1 is lost (209). This is an interesting parallel to my findings that Fpn removal is delayed in cells expressing CA Rab5 (Fig 12) and also that Fpn is present on Rab5-positive phagosomes at 9 min (Fig 11) but not on PI(3)P-positive phagosomes at 10 min (Fig 8). Furthermore, APPL1 has been implicated in regulating trafficking of EGFR (207). Based on this evidence, APPL1 is a plausible candidate as a mediator of Fpn trafficking.

Long term, it would be interesting to investigate if macrophages purposely remove Fpn from the phagosomal membrane to prevent iron supplementation to phagocytosed bacteria. Once mediators of Fpn trafficking are identified, presumably I could modulate Fpn localization to remain at the phagosomal membrane, possibly using dominant-negative constructs or RNA interference. Measurements of iron content in the

phagosome and inquiry into the rate of replication of intraphagosomal bacteria could be compared between Fpn-negative and Fpn-positive phagosomes to more clearly delineate the role Fpn removal plays in nutritional immunity.

In summary, this study demonstrates that macrophages remove Fpn from the phagosomal membrane, likely to prevent extrusion of iron into the phagosomal lumen and thereby help limit bacterial growth inside the phagosome. This finding represents yet another possible mechanism whereby host cells restrict nutrient availability. Future work is needed to more clearly define the trafficking mechanism of Fpn internalized via phagocytosis to provide a more complete understanding of host innate immunity.

REFERENCES

1. Turvey, S. E., and Broide, D. H. (2010) Innate immunity. *J. Allergy Clin. Immunol.* **125**, S24-32
2. Thaiss, C. A., Zmora, N., Levy, M., and Elinav, E. (2016) The microbiome and innate immunity. *Nature.* **535**, 65–74
3. Ricklin, D., Hajishengallis, G., Yang, K., and Lambris, J. D. (2010) Complement: a key system for immune surveillance and homeostasis. *Nat. Immunol.* **11**, 785–797
4. Hood, M. I., and Skaar, E. P. (2012) Nutritional immunity: transition metals at the pathogen-host interface. *Nat. Rev. Microbiol.* **10**, 525–537
5. Flannagan, R. S., Cosío, G., and Grinstein, S. (2009) Antimicrobial mechanisms of phagocytes and bacterial evasion strategies. *Nat. Rev. Microbiol.* **7**, 355–366
6. Stecher, B., and Hardt, W. D. (2008) The role of microbiota in infectious disease. *Trends Microbiol.* **16**, 107–114
7. Weinberg, E. D. (1974) Iron and susceptibility to infectious disease. *Science.* **184**, 952–956
8. Morgan, J. W., and Anders, E. (1980) Chemical composition of Earth, Venus, and Mercury. *Proc. Natl. Acad. Sci. U. S. A.* **77**, 6973–7
9. Posey, J. E., and Gherardini, F. C. (2000) Lack of a role for iron in the Lyme disease pathogen. *Science.* **288**, 1651–3
10. Netz, D. J. A., Stith, C. M., Stümpfig, M., Köpf, G., Vogel, D., Genau, H. M., Stodola, J. L., Lill, R., Burgers, P. M. J., and Pierik, A. J. (2012) Eukaryotic DNA polymerases require an iron-sulfur cluster for the formation of active complexes. *Nat. Chem. Biol.* **8**, 125–132
11. Renton, F. J., and Jeitner, T. M. (1996) Cell cycle-dependent inhibition of the proliferation of human neural tumor cell lines by iron chelators. *Biochem. Pharmacol.* **51**, 1553–61
12. Pauling, L., and Coryell, C. D. (1936) The magnetic properties and structure of hemoglobin, oxyhemoglobin and carbonmonoxyhemoglobin. *Proc. Natl. Acad. Sci. U. S. A.* **22**, 210–6
13. Paoli, M., Anderson, B. F., Baker, H. M., Morgan, W. T., Smith, A., and Baker, E. N. (1999) Crystal structure of hemopexin reveals a novel high-affinity heme site formed between two b-propeller domains. *Nat. Struct. Biol.* **6**, 926–931
14. Paoli, M., Marles-Wright, J., and Smith, A. (2002) Structure–function relationships in heme-proteins. *DNA Cell Biol.* **21**, 271–280
15. Johnson, D. C., Dean, D. R., Smith, A. D., and Johnson, M. K. (2005) Structure, function, and formation of biological iron-sulfur clusters. *Annu. Rev. Biochem.* **74**, 247–281
16. Zhang, J., Frerman, F. E., and Kim, J.-J. P. (2006) Structure of electron transfer flavoprotein-ubiquinone oxidoreductase and electron transfer to the mitochondrial ubiquinone pool. *Proc. Natl. Acad. Sci. U. S. A.* **103**, 16212–7
17. Harrison, P. M., and Arosio, P. (1996) The ferritins: molecular properties, iron storage function and cellular regulation. *Biochim. Biophys. Acta.* **1275**, 161–203
18. Asano, T., Komatsu, M., Yamaguchi-Iwai, Y., Ishikawa, F., Mizushima, N., and Iwai, K. (2011) Distinct mechanisms of ferritin delivery to lysosomes in iron-depleted and iron-replete cells. *Mol. Cell. Biol.* **31**, 2040–2052

19. Gkouvatzos, K., Papanikolaou, G., and Pantopoulos, K. (2012) Regulation of iron transport and the role of transferrin. *Biochim. Biophys. Acta - Gen. Subj.* **1820**, 188–202
20. Aisen, P., Leibman, A., and Zweier, J. (1978) Stoichiometric and site characteristics of the binding of iron to human transferrin. *J Biol Chem.* **253**, 1930–1937
21. Imlay, J. A., Chin, S. M., and Linn, S. (1988) Toxic DNA damage by hydrogen peroxide through the Fenton reaction in vivo and in vitro. *Science.* **240**, 640–2
22. Fenton, H. J. H. (1894) Oxidation of tartaric acid in the presence of iron. *J. Chem. Soc.* **65**, 899–910
23. Asad, N. R., and Leitão, A. C. (1991) Effects of metal ion chelators on DNA strand breaks and inactivation produced by hydrogen peroxide in *Escherichia coli*: detection of iron-independent lesions. *J. Bacteriol.* **173**, 2562–8
24. Nunoshiba, T., Obata, F., Boss, A. C., Oikawa, S., Mori, T., Kawanishi, S., and Yamamoto, K. (1999) Role of iron and superoxide for generation of hydroxyl radical, oxidative DNA lesions, and mutagenesis in *Escherichia coli*. *J. Biol. Chem.* **274**, 34832–34837
25. Rice-Evans, C., and Baysal, E. (1987) Iron-mediated oxidative stress in erythrocytes. *Biochem. J.* **244**, 191–196
26. Dixon, S. J., and Stockwell, B. R. (2013) The role of iron and reactive oxygen species in cell death. *Nat. Chem. Biol.* **10**, 9–17
27. Fleming, M., Trenor, C., Su, M. A., Foernzler, D., Beier, D. R., Dietrich, W. F., and Andrews, N. C. (1997) Microcytic anaemia mice have a mutation in Nramp2, a candidate iron transporter gene. *Nat. Genet.* **16**, 383–386
28. Gunshin, H., Mackenzie, B., Berger, U. V., Gunshin, Y., Romero, M. F., Boron, W. F., Nussberger, S., Gollan, J. L., and Hediger, M. A. (1997) Cloning and characterization of a mammalian proton-coupled metal-ion transporter. *Nature.* **388**, 482–488
29. Shayeghi, M., Latunde-Dada, G. O., Oakhill, J. S., Laftah, A. H., Takeuchi, K., Halliday, N., Khan, Y., Warley, A., McCann, F. E., Hider, R. C., Frazer, D. M., Anderson, G. J., Vulpe, C. D., Simpson, R. J., and McKie, A. T. (2005) Identification of an intestinal heme transporter. *Cell.* **122**, 789–801
30. Laftah, A. H., Latunde-Dada, G. O., Fakih, S., Hider, R. C., Simpson, R. J., and McKie, A. T. (2009) Haem and folate transport by proton-coupled folate transporter/haem carrier protein 1 (SLC46A1). *Br. J. Nutr.* **101**, 1150
31. Le Blanc, S., Garrick, M. D., and Arredondo, M. (2012) Heme carrier protein 1 transports heme and is involved in heme-Fe metabolism. *Am. J. Physiol. Cell Physiol.* **302**, C1780-5
32. Lane, D. J. R., and Richardson, D. R. (2014) Chaperone turns gatekeeper: PCBP2 and DMT1 form an iron-transport pipeline. *Biochem. J.*
33. Yanatori, I., Yasui, Y., Tabuchi, M., and Kishi, F. (2014) Chaperone protein involved in transmembrane transport of iron. *Biochem. J.* **462**, 25–37
34. Donovan, A., Brownlie, A., Zhou, Y., Shepard, J., Pratt, S. J., Moynihan, J., Paw, B. H., Drejer, A., Barut, B., Zapata, A., Law, T. C., Brugnara, C., Lux, S. E., Pinkus, G. S., Pinkus, J. L., Kingsley, P. D., Palis, J., Fleming, M. D., Andrews, N. C., and Zon, L. I. (2000) Positional cloning of zebrafish ferroportin1 identifies a

- conserved vertebrate iron exporter. *Nature*. **403**, 776–81
35. McKie, A. T., Marciani, P., Rolfs, A., Brennan, K., Wehr, K., Barrow, D., Miret, S., Bomford, A., Peters, T. J., Farzaneh, F., Hediger, M. A., Hentze, M. W., and Simpson, R. J. (2000) A novel duodenal iron-regulated transporter, IREG1, implicated in the basolateral transfer of iron to the circulation. *Mol. Cell*. **5**, 299–309
 36. Abboud, S., and Haile, D. J. (2000) A novel mammalian iron-regulated protein involved in intracellular iron metabolism. *J. Biol. Chem*. **275**, 19906–12
 37. Canonne-Hergaux, F., Gruenheid, S., Ponka, P., and Gros, P. (1999) Cellular and subcellular localization of the Nramp2 iron transporter in the intestinal brush border and regulation by dietary iron. *Blood*. **93**, 4406–17
 38. Nemeth, E., Tuttle, M. S., Powelson, J., Vaughn, M. B., Ward, D. M., Ganz, T., Kaplan, J., Donovan, A., Ward, D. M., Ganz, T., and Kaplan, J. (2004) Hepcidin regulates cellular iron efflux by binding to ferroportin and inducing its internalization. *Science*. **306**, 2090–2093
 39. Ganz, T. (2003) Hepcidin, a key regulator of iron metabolism and mediator of anemia of inflammation. *Blood*. **102**, 783–788
 40. Ganz, T. (2012) Macrophages and systemic iron homeostasis. *J. Innate Immun*. **4**, 446–453
 41. Finch, C. A. (1959) Body iron exchange in man. *J. Clin. Invest*. **38**, 392–396
 42. Delaby, C., Pilard, N., Gonçalves, A. S., Beaumont, C., and Canonne-Hergaux, F. (2005) Presence of the iron exporter ferroportin at the plasma membrane of macrophages is enhanced by iron loading and down-regulated by hepcidin. *Blood*. **106**, 3979–3984
 43. Nemeth, E., and Ganz, T. (2009) The role of hepcidin in iron metabolism. *Acta Haematol*. **122**, 78–86
 44. Ganz, T. (2003) Hepcidin, a key regulator of iron metabolism and mediator of anemia of inflammation. *Blood*. **102**, 783–8
 45. Zimmermann, M. B., and Hurrell, R. F. (2007) Nutritional iron deficiency. *Lancet*. **370**, 511–520
 46. Badal, S., Her, Y. F., and Maher, L. J. (2015) Nonantibiotic effects of Fluoroquinolones in mammalian cells. *J. Biol. Chem*. **290**, 22287–97
 47. Shander, A., Cappellini, M. D., and Goodnough, L. T. (2009) Iron overload and toxicity: the hidden risk of multiple blood transfusions. *Vox Sang*. **97**, 185–197
 48. Feder, J. N., Gnirke, A., Thomas, W., Tsuchihashi, Z., Ruddy, D. A., Basava, A., Dormishian, F., Domingo, R., Ellis, M. C., Fullan, A., Hinton, L. M., Jones, N. L., Kimmel, B. E., Kronmal, G. S., Lauer, P., Lee, V. K., Loeb, D. B., Mapa, F. A., McClelland, E., Meyer, N. C., Mintier, G. A., Moeller, N., Moore, T., Morikang, E., Prass, C. E., Quintana, L., Starnes, S. M., Schatzman, R. C., Brunke, K. J., Drayna, D. T., Risch, N. J., Bacon, B. R., and Wolff, R. K. (1996) A novel MHC class I-like gene is mutated in patients with hereditary haemochromatosis. *Nat. Genet*. **13**, 399–408
 49. Pigeon, C., Ilyin, G., Courselaud, B., Leroyer, P., Turlin, B., Brissot, P., and Loréal, O. (2001) A new mouse liver-specific gene, encoding a protein homologous to human antimicrobial peptide hepcidin, is overexpressed during iron overload. *J. Biol. Chem*. **276**, 7811–9

50. Camaschella, C., Roetto, A., Cali, A., De Gobbi, M., Garozzo, G., Carella, M., Majorano, N., Totaro, A., and Gasparini, P. (2000) The gene TFR2 is mutated in a new type of haemochromatosis mapping to 7q22. *Nat. Genet.* **25**, 14–15
51. Njajou, O. T., Vaessen, N., Joosse, M., Berghuis, B., van Dongen, J. W. F., Breuning, M. H., Snijders, P. J. L. M., Rutten, W. P. F., Sandkuijl, L. A., Oostra, B. A., van Duijn, C. M., and Heutink, P. (2001) A mutation in SLC11A3 is associated with autosomal dominant hemochromatosis. *Nat. Genet.* **28**, 213–214
52. Montosi, G., Donovan, A., Totaro, A., Garuti, C., Pignatti, E., Cassanelli, S., Trenor, C. C., Gasparini, P., Andrews, N. C., and Pietrangelo, A. (2001) Autosomal-dominant hemochromatosis is associated with a mutation in the ferroportin (SLC11A3) gene. *J. Clin. Invest.* **108**, 619–23
53. Barton, J. C., and Acton, R. T. (2009) Hemochromatosis and *Vibrio vulnificus* wound infections. *J. Clin. Gastroenterol.* **43**, 890–893
54. Thwaites, P. A., and Woods, M. L. (2017) Sepsis and siderosis, *Yersinia enterocolitica* and hereditary haemochromatosis. *BMJ Case Rep.* **2017**, bcr2016218185
55. Khan, F. A., Fisher, M. A., and Khakoo, R. A. (2007) Association of hemochromatosis with infectious diseases: expanding spectrum. *Int. J. Infect. Dis. IJID Off. Publ. Int. Soc. Infect. Dis.* **11**, 482–487
56. Vento, S., Cainelli, F., and Cesario, F. (2006) Infections and thalassaemia. *Lancet Infect. Dis.* **6**, 226–233
57. Adamkiewicz, T. V., Berkovitch, M., Krishnan, C., Polsinelli, C., Kermack, D., and Olivieri, N. F. (1998) Infection due to *Yersinia enterocolitica* in a series of patients with beta-thalassemia: incidence and predisposing factors. *Clin. Infect. Dis. An Off. Publ. Infect. Dis. Soc. Am.* **27**, 1362–1366
58. Sheldon, J. R., and Heinrichs, D. E. (2015) Recent developments in understanding the iron acquisition strategies of gram positive pathogens. *FEMS Microbiol. Rev.* **39**, 592–630
59. Troxell, B., and Hassan, H. M. (2013) Transcriptional regulation by Ferric Uptake Regulator (Fur) in pathogenic bacteria. *Front. Cell. Infect. Microbiol.* **3**, 59
60. Torres, V. J., Attia, A. S., Mason, W. J., Hood, M. I., Corbin, B. D., Beasley, F. C., Anderson, K. L., Stauff, D. L., McDonald, W. H., Zimmerman, L. J., Friedman, D. B., Heinrichs, D. E., Dunman, P. M., and Skaar, E. P. (2010) *Staphylococcus aureus fur* regulates the expression of virulence factors that contribute to the pathogenesis of pneumonia. *Infect Immun.* **78**, 1618–1628
61. Pishchany, G., Sheldon, J. R., Dickson, C. F., Alam, M. T., Read, T. D., Gell, D. A., Heinrichs, D. E., and Skaar, E. P. (2014) IsdB-dependent hemoglobin binding is required for acquisition of heme by *Staphylococcus aureus*. *J. Infect. Dis.* **209**, 1764–1772
62. Robey, M., and Cianciotto, N. P. (2002) *Legionella pneumophila feoAB* promotes ferrous iron uptake and intracellular infection. *Infect. Immun.* **70**, 5659–5669
63. Aranda, J., Cortés, P., Garrido, M. E., Fittipaldi, N., Llagostera, M., Gottschalk, M., and Barbé, J. (2009) Contribution of the FeoB transporter to *Streptococcus suis* virulence. *Int. Microbiol. Off. J. Spanish Soc. Microbiol.* **12**, 137–143
64. Stojiljkovic, I., and Perkins-Balding, D. (2002) Processing of heme and heme-containing proteins by bacteria. *DNA Cell Biol.* **21**, 281–295

65. Vandenesch, F., Lina, G., and Henry, T. (2012) *Staphylococcus aureus* hemolysins, bi-component leukocidins, and cytolytic peptides: A redundant arsenal of membrane-damaging virulence factors? *Front. Cell. Infect. Microbiol.* **2**, 12
66. Cope, L. D., Thomas, S. E., Hrkal, Z., and Hansen, E. J. (1998) Binding of heme-hemopexin complexes by soluble HxuA protein allows utilization of this complexed heme by *Haemophilus influenzae*. *Infect. Immun.* **66**, 4511–4516
67. Bai, X., Teng, D., Tian, Z., Zhu, Y., Yang, Y., and Wang, J. (2010) Contribution of bovine lactoferrin inter-lobe region to iron binding stability and antimicrobial activity against *Staphylococcus aureus*. *Biometals*. 10.1007/s10534-010-9300-x
68. Aguila, A., Herrera, A. G., Morrison, D., Cosgrove, B., Perojo, A., Montesinos, I., Perez, J., Sierra, G., Gemmell, C. G., and Brock, J. H. (2001) Bacteriostatic activity of human lactoferrin against *Staphylococcus aureus* is a function of its iron-binding properties and is not influenced by antibiotic resistance. *FEMS Immunol Med Microbiol.* **31**, 145–152
69. Arnold, R. R., Brewer, M., and Gauthier, J. J. (1980) Bactericidal activity of human lactoferrin: sensitivity of a variety of microorganisms. *Infect. Immun.* **28**, 893–8
70. Goetz, D. H., Holmes, M. A., Borregaard, N., Blumh, M. E., Raymond, K. N., and Strong, R. K. (2002) The neutrophil lipocalin NGAL is a bacteriostatic agent that interferes with siderophore-mediated iron acquisition. *Mol. Cell.* **10**, 1033–1043
71. Vidal, S. M., Malo, D., Vogan, K., Skamene, E., and Gros, P. (1993) Natural resistance to infection with intracellular parasites: Isolation of a candidate for Bcg. *Cell.* **73**, 469–485
72. Forbes, J. R., and Gros, P. (2001) Divalent-metal transport by NRAMP proteins at the interface of host-pathogen interactions. *Trends Microbiol.* **9**, 397–403
73. Hedges, J. F., Kimmel, E., Snyder, D. T., Jerome, M., and Jutila, M. A. (2013) Solute Carrier 11A1 is expressed by innate lymphocytes and augments their activation. *J. Immunol.* **190**, 4263–4273
74. Gruenheid, S., Pinner, E., Desjardins, M., and Gros, P. (1997) Natural resistance to infection with intracellular pathogens: the Nramp1 protein is recruited to the membrane of the phagosome. *J. Exp. Med.* **185**, 717–730
75. Wessling-Resnick, M. (2015) Nramp1 and other transporters involved in metal withholding during infection. *J. Biol. Chem.* **290**, 18984–90
76. Jabado, N., Jankowski, a, Dougaparsad, S., Picard, V., Grinstein, S., and Gros, P. (2000) Natural resistance to intracellular infections: natural resistance-associated macrophage protein 1 (Nramp1) functions as a pH-dependent manganese transporter at the phagosomal membrane. *J. Exp. Med.* **192**, 1237–1248
77. Atkinson, P. G., and Barton, C. H. (1999) High level expression of Nramp1G169 in RAW264.7 cell transfectants: analysis of intracellular iron transport. *Immunology.* **96**, 656–62
78. Goswami, T., Bhattacharjee, A., Babal, P., Searle, S., Moore, E., Li, M., and Blackwell, J. M. (2001) Natural-resistance-associated macrophage protein 1 is an H⁺/bivalent cation antiporter. *Biochem. J.* **354**, 511–9
79. Tabuchi, M., Yoshimori, T., Yamaguchi, K., Yoshida, T., and Kishi, F. (2000) Human NRAMP2/DMT1, which mediates iron transport across endosomal membranes, is localized to late endosomes and lysosomes in HEp-2 cells. *J. Biol.*

- Chem.* **275**, 22220–8
80. Picard, V., Govoni, G., Jabado, N., and Gros, P. (2000) Nramp 2 (DCT1/DMT1) expressed at the plasma membrane transports iron and other divalent cations into a calcein-accessible cytoplasmic pool. *J. Biol. Chem.* **275**, 35738–45
 81. Owusu-Boaitey, N., Bauckman, K. A., Zhang, T., and Mysorekar, I. U. (2016) Macrophagic control of the response to uropathogenic *E. coli* infection by regulation of iron retention in an IL-6-dependent manner. *Immunity, Inflamm. Dis.* **4**, 413–426
 82. Arezes, J., Jung, G., Gabayan, V., Valore, E., Ruchala, P., Gulig, P. A. A., Ganz, T., Nemeth, E., and Bulut, Y. (2015) Hepcidin-induced hypoferremia is a critical host defense mechanism against the siderophilic bacterium *Vibrio vulnificus*. *Cell Host Microbe.* **17**, 47–57
 83. Northrop-Clewes, C. A. (2008) Interpreting indicators of iron status during an acute phase response – lessons from malaria and human immunodeficiency virus. *Ann. Clin. Biochem.* **45**, 18–32
 84. Inaoka, T., Matsumura, Y., and Tsuchido, T. (1999) SodA and manganese are essential for resistance to oxidative stress in growing and sporulating cells of *Bacillus subtilis*. *J. Bacteriol.* **181**, 1939–1943
 85. Kehl-Fie, T. E., and Skaar, E. P. (2010) Nutritional immunity beyond iron: a role for manganese and zinc. *Curr Opin Chem Biol.* **14**, 218–224
 86. Wąty, J., Potocki, S., and Rowińska-Żyrek, M. (2016) Zinc homeostasis at the bacteria/host interface-from coordination chemistry to nutritional immunity. *Chem. - A Eur. J.* **22**, 15992–16010
 87. Brophy, M. B., and Nolan, E. M. (2015) Manganese and microbial pathogenesis: sequestration by the mammalian immune system and utilization by microorganisms. *ACS Chem. Biol.* **10**, 641–651
 88. Damo, S. M., Kehl-Fie, T. E., Sugitani, N., Holt, M. E., Rathi, S., Murphy, W. J., Zhang, Y., Betz, C., Hench, L., Fritz, G., Skaar, E. P., and Chazin, W. J. (2013) Molecular basis for manganese sequestration by calprotectin and roles in the innate immune response to invading bacterial pathogens. *Proc. Natl. Acad. Sci. U. S. A.* **110**, 3841–3846
 89. Corbin, B. D., Seeley, E. H., Raab, A., Feldmann, J., Miller, M. R., Torres, V. J., Anderson, K. L., Dattilo, B. M., Dunman, P. M., Gerads, R., Caprioli, R. M., Nacken, W., Chazin, W. J., and Skaar, E. P. (2008) Metal chelation and inhibition of bacterial growth in tissue abscesses. *Science.* **319**, 962–965
 90. Urban, C. F., Ermert, D., Schmid, M., Abu-Abed, U., Goosmann, C., Nacken, W., Brinkmann, V., Jungblut, P. R., and Zychlinsky, A. (2009) Neutrophil extracellular traps contain calprotectin, a cytosolic protein complex involved in host defense against *Candida albicans*. *PLoS Pathog.* **5**, e1000639
 91. Clark, H. L., Jhingran, A., Sun, Y., Vareechon, C., de Jesus Carrion, S., Skaar, E. P., Chazin, W. J., Calera, J. A., Hohl, T. M., and Pearlman, E. (2015) Zinc and manganese chelation by neutrophil S100A8/A9 (Calprotectin) limits extracellular *Aspergillus fumigatus* hyphal growth and corneal infection. *J. Immunol.*
 92. Gläser, R., Harder, J., Lange, H., Bartels, J., Christophers, E., and Schröder, J.-M. (2005) Antimicrobial psoriasin (S100A7) protects human skin from *Escherichia coli* infection. *Nat. Immunol.* **6**, 57–64

93. Hattori, F., Kiatsurayanon, C., Okumura, K., Ogawa, H., Ikeda, S., Okamoto, K., and Niyonsaba, F. (2014) The antimicrobial protein S100A7/psoriasin enhances the expression of keratinocyte differentiation markers and strengthens the skin's tight junction barrier. *Br. J. Dermatol.* **171**, 742–753
94. Haley, K. P., Delgado, A. G., Piazuolo, M. B., Mortensen, B. L., Correa, P., Damo, S. M., Chazin, W. J., Skaar, E. P., and Gaddy, J. A. (2015) The human antimicrobial protein Calgranulin C participates in control of *Helicobacter pylori* growth and regulation of virulence. *Infect. Immun.* **83**, 2944–56
95. Cunden, L. S., Gaillard, A., and Nolan, E. M. (2016) Calcium ions tune the zinc-sequestering properties and antimicrobial activity of human S100A12. *Chem. Sci.* **7**, 1338–1348
96. Lu, J., Buse, H. Y., Gomez-Alvarez, V., Struewing, I., Santo Domingo, J., and Ashbolt, N. J. (2014) Impact of drinking water conditions and copper materials on downstream biofilm microbial communities and *Legionella pneumophila* colonization. *J. Appl. Microbiol.* **117**, 905–918
97. Elguindi, J., Hao, X., Lin, Y., Alwathnani, H. A., Wei, G., and Rensing, C. (2011) Advantages and challenges of increased antimicrobial copper use and copper mining. *Appl. Microbiol. Biotechnol.* **91**, 237–249
98. Monk, A. B., Kanmukhla, V., Trinder, K., and Borkow, G. (2014) Potent bactericidal efficacy of copper oxide impregnated non-porous solid surfaces. *BMC Microbiol.* **14**, 57
99. White, C., Lee, J., Kambe, T., Fritsche, K., and Petris, M. J. (2009) A role for the ATP7A copper-transporting ATPase in macrophage bactericidal activity. *J. Biol. Chem.* **284**, 33949–33956
100. Nose, Y., Wood, L. K., Kim, B.-E., Prohaska, J. R., Fry, R. S., Spears, J. W., and Thiele, D. J. (2010) Ctr1 is an apical copper transporter in mammalian intestinal epithelial cells in vivo that is controlled at the level of protein stability. *J. Biol. Chem.* **285**, 32385–32392
101. Lutsenko, S., Gupta, A., Burkhead, J. L., and Zuzel, V. (2008) Cellular multitasking: The dual role of human Cu-ATPases in cofactor delivery and intracellular copper balance. *Arch. Biochem. Biophys.* **476**, 22–32
102. Hamza, I., Prohaska, J., and Gitlin, J. D. (2003) Essential role for Atox1 in the copper-mediated intracellular trafficking of the Menkes ATPase. *Proc. Natl. Acad. Sci. U. S. A.* **100**, 1215–1220
103. Wolschendorf, F., Ackart, D., Shrestha, T. B., Hascall-Dove, L., Nolan, S., Lamichhane, G., Wang, Y., Bossmann, S. H., Basaraba, R. J., and Niederweis, M. (2011) Copper resistance is essential for virulence of *Mycobacterium tuberculosis*. *Proc. Natl. Acad. Sci. U. S. A.* **108**, 1621–6
104. Mitchell, C. J., Shawki, A., Ganz, T., Nemeth, E., and Mackenzie, B. (2014) Functional properties of human ferroportin, a cellular iron exporter reactive also with cobalt and zinc. *Am. J. Physiol. - Cell Physiol.*
105. Madejczyk, M. S., and Ballatori, N. (2012) The iron transporter ferroportin can also function as a manganese exporter. *Biochim. Biophys. Acta - Biomembr.* **1818**, 651–657
106. Drakesmith, H., Nemeth, E., and Ganz, T. (2015) Ironing out Ferroportin. *Cell Metab.* **22**, 777–787

107. Donovan, A., Lima, C. A., Pinkus, J. L., Pinkus, G. S., Zon, L. I., Robine, S., and Andrews, N. C. (2005) The iron exporter ferroportin/Slc40a1 is essential for iron homeostasis. *Cell Metab.* **1**, 191–200
108. Schimanski, L. M., Drakesmith, H., Merryweather-Clarke, A. T., Viprakasit, V., Edwards, J. P., Sweetland, E., Bastin, J. M., Cowley, D., Chinthammitr, Y., Robson, K. J. H., and Townsend, A. R. M. (2005) In vitro functional analysis of human ferroportin (FPN) and hemochromatosis-associated FPN mutations. *Blood.* **105**, 4096–102
109. Gonçalves, A. S., Muzeau, F., Blaybel, R., Hetet, G., Driss, F., Delaby, C., Canonne-Hergaux, F., and Beaumont, C. (2006) Wild-type and mutant ferroportins do not form oligomers in transfected cells. *Biochem. J.* **396**, 265–75
110. Liu, X.-B., Yang, F., and Haile, D. J. Functional consequences of ferroportin 1 mutations. *Blood Cells. Mol. Dis.* **35**, 33–46
111. De Domenico, I., Ward, D. M., Musci, G., and Kaplan, J. (2007) Evidence for the multimeric structure of ferroportin. *Blood.* **109**, 2205–9
112. Wallace, D. F., Harris, J. M., and Subramaniam, V. N. (2010) Functional analysis and theoretical modeling of ferroportin reveals clustering of mutations according to phenotype. *AJP Cell Physiol.* **298**, C75–C84
113. Le Gac, G., Ka, C., Joubrel, R., Gourlaouen, I., Lehn, P., Mornon, J.-P., Férec, C., and Callebaut, I. (2013) Structure-function analysis of the human ferroportin iron exporter (SLC40A1): effect of hemochromatosis type 4 disease mutations and identification of critical residues. *Hum. Mutat.* **34**, 1371–80
114. Bonaccorsi di Patti, M. C., Polticelli, F., Cece, G., Cutone, A., Felici, F., Persichini, T., and Musci, G. (2014) A structural model of human ferroportin and of its iron binding site. *FEBS J.* **281**, 2851–60
115. Taniguchi, R., Kato, H. E., Font, J., Deshpande, C. N., Wada, M., Ito, K., Ishitani, R., Jormakka, M., and Nureki, O. (2015) Outward- and inward-facing structures of a putative bacterial transition-metal transporter with homology to ferroportin. *Nat. Commun.* **6**, 8545
116. Bonaccorsi di Patti, M. C., Polticelli, F., Tortosa, V., Furbetta, P. A., and Musci, G. (2015) A bacterial homologue of the human iron exporter ferroportin. *FEBS Lett.* **589**, 3829–3835
117. Yanatori, I., Richardson, D. R., Imada, K., and Kishi, F. (2016) Iron export through the transporter ferroportin 1 is modulated by the iron chaperone PCBP2. *J. Biol. Chem.* **291**, 17303–18
118. Eid, C., Hémadi, M., Ha-Duong, N.-T., and El Hage Chahine, J.-M. (2014) Iron uptake and transfer from ceruloplasmin to transferrin. *Biochim. Biophys. Acta.* **1840**, 1771–1781
119. Marro, S., Chiabrando, D., Messina, E., Stolte, J., Turco, E., Tolosano, E., and Muckenthaler, M. U. (2010) Heme controls ferroportin1 (FPN1) transcription involving Bach1, Nrf2 and a MARE/ARE sequence motif at position -7007 of the FPN1 promoter. *Haematologica.* **95**, 1261–8
120. Harada, N., Kanayama, M., Maruyama, A., Yoshida, A., Tazumi, K., Hosoya, T., Mimura, J., Toki, T., Maher, J. M., Yamamoto, M., and Itoh, K. (2011) Nrf2 regulates ferroportin 1-mediated iron efflux and counteracts lipopolysaccharide-induced ferroportin 1 mRNA suppression in macrophages. *Arch. Biochem.*

- Biophys.* **508**, 101–109
121. Nairz, M., Schleicher, U., Schroll, A., Sonnweber, T., Theurl, I., Ludwiczek, S., Talasz, H., Brandacher, G., Moser, P. L., Muckenthaler, M. U., Fang, F. C., Bogdan, C., and Weiss, G. (2013) Nitric oxide-mediated regulation of ferroportin-1 controls macrophage iron homeostasis and immune function in *Salmonella* infection. *J. Exp. Med.* **275**, 19906
 122. Lymboussaki, A., Pignatti, E., Montosi, G., Garuti, C., Haile, D. J., and Pietrangelo, A. (2003) The role of the iron responsive element in the control of ferroportin1/IREG1/MTP1 gene expression. *J. Hepatol.* **39**, 710–5
 123. Ganz, T. (2005) Heparin--a regulator of intestinal iron absorption and iron recycling by macrophages. *Best Pr. Res Clin Haematol.* **18**, 171–182
 124. Qiao, B., Sugianto, P., Fung, E., Del-Castillo-Rueda, A., Moran-Jimenez, M. J., Ganz, T., and Nemeth, E. (2012) Heparin-induced endocytosis of ferroportin is dependent on ferroportin ubiquitination. *Cell Metab.* **15**, 918–924
 125. De Domenico, I., Ward, D. M., Langelier, C., Vaughn, M. B., Nemeth, E., Sundquist, W. I., Ganz, T., Musci, G., and Kaplan, J. (2007) The molecular mechanism of heparin-mediated ferroportin down-regulation. *Mol. Biol. Cell.* **18**, 2569–78
 126. De Domenico, I., Ward, D. M., Nemeth, E., Vaughn, M. B., Musci, G., Ganz, T., and Kaplan, J. (2005) The molecular basis of ferroportin-linked hemochromatosis. *Proc. Natl. Acad. Sci. U. S. A.* **102**, 8955–60
 127. Fernandes, A., Preza, G. C., Phung, Y., De Domenico, I., Kaplan, J., Ganz, T., and Nemeth, E. (2009) The molecular basis of heparin-resistant hereditary hemochromatosis. *Blood*
 128. Pietrangelo, A. (2004) The ferroportin disease. *Blood Cells, Mol. Dis.* **32**, 131–138
 129. Brown, D. E., Nick, H. J., McCoy, M. W., Moreland, S. M., Stepanek, A. M., Benik, R., O'Connell, K. E., Pilonieta, M. C., Nagy, T. A., and Detweiler, C. S. (2015) Increased Ferroportin-1 expression and rapid splenic iron loss occur with anemia caused by *Salmonella enterica* Serovar Typhimurium infection in mice. *Infect. Immun.* **83**, 2290–2299
 130. Haschka, D., Nairz, M., Demetz, E., Wienerroither, S., Decker, T., and Weiss, G. (2015) Contrasting regulation of macrophage iron homeostasis in response to infection with *Listeria monocytogenes* depending on localization of bacteria. *Metallomics.* **7**, 1036–45
 131. Johnson, E. E., Sandgren, A., Cherayil, B. J., Murray, M., and Wessling-Resnick, M. (2010) Role of ferroportin in macrophage-mediated immunity. *Infect. Immun.* **78**, 5099–106
 132. Van Zandt, K. E., Sow, F. B., Florence, W. C., Zwilling, B. S., Satoskar, A. R., Schlesinger, L. S., and Lafuse, W. P. (2008) The iron export protein ferroportin 1 is differentially expressed in mouse macrophage populations and is present in the mycobacterial-containing phagosome. *J. Leukoc. Biol.* **84**, 689–700
 133. Murray, P. J., and Wynn, T. A. (2011) Protective and pathogenic functions of macrophage subsets. *Nat. Rev. Immunol.* **11**, 723–37
 134. Freeman, S. A., and Grinstein, S. (2014) Phagocytosis: receptors, signal integration, and the cytoskeleton. *Immunol. Rev.* **262**, 193–215
 135. Crane, M. J., Hokeness-Antonelli, K. L., and Salazar-Mather, T. P. (2009)

- Regulation of inflammatory monocyte/macrophage recruitment from the bone marrow during murine cytomegalovirus infection: role for type I interferons in localized induction of CCR2 ligands. *J. Immunol.* **183**, 2810–7
136. Shi, C., and Pamer, E. G. (2011) Monocyte recruitment during infection and inflammation. *Nat. Rev. Immunol.* **11**, 762–74
 137. Wang, N., Liang, H., and Zen, K. (2014) Molecular mechanisms that influence the macrophage M1-M2 polarization balance. *Front. Immunol.* **5**, 614
 138. Sica, A., and Mantovani, A. (2012) Macrophage plasticity and polarization: in vivo veritas. *J. Clin. Invest.* **122**, 787–795
 139. Canton, J. (2014) Phagosome maturation in polarized macrophages. *J. Leukoc. Biol.* **96**, 729–38
 140. Flannagan, R. S., Harrison, R. E., Yip, C. M., Jaqaman, K., and Grinstein, S. (2010) Dynamic macrophage “probing” is required for the efficient capture of phagocytic targets. *J. Cell Biol.* **191**, 1205–1218
 141. Flannagan, R. S., Jaumouillé, V., and Grinstein, S. (2012) The cell biology of phagocytosis. *Annu. Rev. Pathol.* **7**, 61–98
 142. Sobota, A., Strzelecka-Kiliszek, A., Gładkowska, E., Yoshida, K., Mrozińska, K., and Kwiatkowska, K. (2005) Binding of IgG-opsonized particles to Fc gamma R is an active stage of phagocytosis that involves receptor clustering and phosphorylation. *J. Immunol.* **175**, 4450–4457
 143. Esteban, A., Popp, M. W., Vyas, V. K., Strijbis, K., Ploegh, H. L., and Fink, G. R. (2011) Fungal recognition is mediated by the association of dectin-1 and galectin-3 in macrophages. *Proc. Natl. Acad. Sci.* **108**, 14270–14275
 144. Jaumouillé, V., Farkash, Y., Jaqaman, K., Das, R., Lowell, C. A., and Grinstein, S. (2014) Actin cytoskeleton reorganization by Syk regulates Fcγ receptor responsiveness by increasing its lateral mobility and clustering. *Dev. Cell.* **29**, 534–546
 145. Dewitt, S., Tian, W., and Hallett, M. B. (2006) Localised PtdIns(3,4,5)P3 or PtdIns(3,4)P2 at the phagocytic cup is required for both phagosome closure and Ca²⁺ signalling in HL60 neutrophils. *J. Cell Sci.* **119**, 443–51
 146. Levin, R., Hammond, G. R. V., Balla, T., De Camilli, P., Fairn, G. D., and Grinstein, S. (2017) Multiphasic dynamics of phosphatidylinositol 4-phosphate during phagocytosis. *Mol. Biol. Cell.* **28**, 128–140
 147. Vieira, O. V., Botelho, R. J., Rameh, L., Brachmann, S. M., Matsuo, T., Davidson, H. W., Schreiber, A., Backer, J. M., Cantley, L. C., and Grinstein, S. (2001) Distinct roles of class I and class III phosphatidylinositol 3-kinases in phagosome formation and maturation. *J. Cell Biol.* **155**, 19–25
 148. Vieira, O. V., Bucci, C., Harrison, R. E., Trimble, W. S., Lanzetti, L., Gruenberg, J., Schreiber, A. D., Stahl, P. D., and Grinstein, S. (2003) Modulation of Rab5 and Rab7 recruitment to phagosomes by phosphatidylinositol 3-kinase. *Mol. Cell. Biol.* **23**, 2501–2514
 149. Huynh, K. K., Eskelinen, E.-L., Scott, C. C., Malevanets, A., Saftig, P., and Grinstein, S. (2007) LAMP proteins are required for fusion of lysosomes with phagosomes. *EMBO J.* **26**, 313–324
 150. Flannagan, R. S., Heit, B., and Heinrichs, D. E. (2015) Antimicrobial mechanisms of macrophages and the immune evasion strategies of *Staphylococcus aureus*.

- Pathogens*. **4**, 826–868
151. Lukacs, G. L., Rotstein, O. D., and Grinstein, S. (1991) Determinants of the phagosomal pH in macrophages. In situ assessment of vacuolar H(+)-ATPase activity, counterion conductance, and H⁺ “leak.” *J. Biol. Chem.* **266**, 24540–24548
 152. Claus, V., Jahraus, A., Tjelle, T., Berg, T., Kirschke, H., Faulstich, H., and Griffiths, G. (1998) Lysosomal enzyme trafficking between phagosomes, endosomes, and lysosomes in J774 macrophages. Enrichment of cathepsin H in early endosomes. *J. Biol. Chem.* **273**, 9842–9851
 153. Müller, S., Faulhaber, A., Sieber, C., Pfeifer, D., Hochberg, T., Gansz, M., Deshmukh, S. D., Dauth, S., Brix, K., Saftig, P., Peters, C., Henneke, P., and Reinheckel, T. (2014) The endolysosomal cysteine cathepsins L and K are involved in macrophage-mediated clearance of *Staphylococcus aureus* and the concomitant cytokine induction. *FASEB J. Off. Publ. Fed. Am. Soc. Exp. Biol.* **28**, 162–175
 154. Yang, Y., Bazhin, A. V., Werner, J., and Karakhanova, S. (2013) Reactive oxygen species in the immune system. *Int. Rev. Immunol.* **32**, 249–270
 155. Connor, M. G., Pulsifer, A. R., Price, C. T., Abu Kwaik, Y., and Lawrenz, M. B. (2015) *Yersinia pestis* requires host Rab1b for survival in macrophages. *PLoS Pathog.* **11**, e1005241
 156. Cano, V., March, C., Insua, J. L., Aguiló, N., Llobet, E., Moranta, D., Regueiro, V., Brennan, G. P., Millán-Lou, M. I., Martín, C., Garmendia, J., and Bengoechea, J. A. (2015) *Klebsiella pneumoniae* survives within macrophages by avoiding delivery to lysosomes. *Cell. Microbiol.* **17**, 1537–60
 157. Vergne, I., Chua, J., and Deretic, V. (2003) Tuberculosis toxin blocking phagosome maturation inhibits a novel Ca²⁺/calmodulin-PI3K hVPS34 cascade. *J. Exp. Med.* **198**, 653–659
 158. Vieira, O. V., Harrison, R. E., Scott, C. C., Stenmark, H., Alexander, D., Liu, J., Gruenberg, J., Schreiber, A. D., and Grinstein, S. (2004) Acquisition of Hrs, an essential component of phagosomal maturation, is impaired by mycobacteria. *Mol. Cell. Biol.* **24**, 4593–4604
 159. Kyei, G. B., Vergne, I., Chua, J., Roberts, E., Harris, J., Junutula, J. R., and Deretic, V. (2006) Rab14 is critical for maintenance of *Mycobacterium tuberculosis* phagosome maturation arrest. *EMBO J.* **25**, 5250–9
 160. Master, S. S., Rampini, S. K., Davis, A. S., Keller, C., Ehlers, S., Springer, B., Timmins, G. S., Sander, P., and Deretic, V. (2008) *Mycobacterium tuberculosis* prevents inflammasome activation. *Cell Host Microbe.* **3**, 224–232
 161. Beauregard, K. E., Lee, K.-D., Collier, R. J., and Swanson, J. A. (1997) pH-dependent perforation of macrophage phagosomes by Listeriolysin O from *Listeria monocytogenes*. *J. Exp. Med.* **186**, 1159–1163
 162. Grant, B. D., and Donaldson, J. G. (2009) Pathways and mechanisms of endocytic recycling. *Nat. Rev. Mol. Cell Biol.* **10**, 597–608
 163. Barr, F. A. (2013) Rab GTPases and membrane identity: Causal or inconsequential? *J. Cell Biol.*
 164. Pereira-Leal, J. B., and Seabra, M. C. (2001) Evolution of the rab family of small GTP-binding proteins. *J. Mol. Biol.* **313**, 889–901
 165. Dautry-Varsat, A., Ciechanover, A., and Lodish, H. F. (1983) pH and the recycling

- of transferrin during receptor-mediated endocytosis. *Proc. Natl. Acad. Sci. U. S. A.* **80**, 2258–2262
166. McCaffrey, M. W., Bielli, A., Cantalupo, G., Mora, S., Roberti, V., Santillo, M., Drummond, F., and Bucci, C. (2001) Rab4 affects both recycling and degradative endosomal trafficking. *FEBS Lett.* **495**, 21–30
 167. Takahashi, S., Kubo, K., Waguri, S., Yabashi, a., Shin, H.-W., Katoh, Y., and Nakayama, K. (2012) Rab11 regulates exocytosis of recycling vesicles at the plasma membrane. *J. Cell Sci.* **125**, 4049–4057
 168. Eden, E. R., White, I. J., and Futter, C. E. (2009) Down-regulation of epidermal growth factor receptor signalling within multivesicular bodies. *Biochem. Soc. Trans.* **37**, 173–7
 169. Babst, M. (2011) MVB vesicle formation: ESCRT-dependent, ESCRT-independent and everything in between. *Curr. Opin. Cell Biol.* **23**, 452–457
 170. Futter, C. E., Pearse, A., Hewlett, L. J., and Hopkins, C. R. (1996) Multivesicular endosomes containing internalized EGF-EGF receptor complexes mature and then fuse directly with lysosomes. *J. Cell Biol.* **132**, 1011–1023
 171. Vanlandingham, P. A., and Ceresa, B. P. (2009) Rab7 regulates late endocytic trafficking downstream of multivesicular body biogenesis and cargo sequestration. *J. Biol. Chem.* **284**, 12110–24
 172. van Dam, E. M., ten Broeke, T., Jansen, K., Spijkers, P., and Stoorvogel, W. (2002) Endocytosed transferrin receptors recycle via distinct dynamin and phosphatidylinositol 3-kinase-dependent pathways. *J. Biol. Chem.* **277**, 48876–48883
 173. Yamauchi, S., Kawauchi, K., and Sawada, Y. (2012) Myosin II-dependent exclusion of CD45 from the site of Fcγ receptor activation during phagocytosis. *FEBS Lett.* **586**, 3229–35
 174. Boles, B. R., and Horswill, A. R. (2008) Agr-mediated dispersal of *Staphylococcus aureus* biofilms. *PLoS Pathog.* **4**, e1000052
 175. Rowland, A. A., Chitwood, P. J., Phillips, M. J., and Voeltz, G. K. (2014) ER contact sites define the position and timing of endosome fission. *Cell.* **159**, 1027–1041
 176. Dröse, S., Bindseil, K. U., Bowman, E. J., Siebers, A., Zeeck, A., and Altendorf, K. (1993) Inhibitory effect of modified bafilomycins and concanamycins on P- and V-type adenosinetriphosphatases. *Biochemistry.* **32**, 3902–6
 177. Dunn, K. W., Kamocka, M. M., and McDonald, J. H. (2011) A practical guide to evaluating colocalization in biological microscopy. *Am. J. Physiol. Cell Physiol.* **300**, C723-42
 178. Bolte, S., and Cordelieres, F. P. (2006) A guided tour into subcellular colocalization analysis in light microscopy. *J. Microsc.* **224**, 213–232
 179. Adler, J., and Parmryd, I. (2007) Letter to the Editor. *J. Microsc.* **227**, 83–83
 180. van der Sluijs, P., Hull, M., Webster, P., Mâle, P., Goud, B., and Mellman, I. (1992) The small GTP-binding protein rab4 controls an early sorting event on the endocytic pathway. *Cell.* **70**, 729–40
 181. Vlahos, C. J., Matter, W. F., Hui, K. Y., and Brown, R. F. (1994) A specific inhibitor of phosphatidylinositol 3-kinase, 2-(4-morpholinyl)-8-phenyl-4H-1-benzopyran-4-one (LY294002). *J. Biol. Chem.* **269**, 5241–8

182. Schlam, D., Bagshaw, R. D., Freeman, S. A., Collins, R. F., Pawson, T., Fairn, G. D., and Grinstein, S. (2015) Phosphoinositide 3-kinase enables phagocytosis of large particles by terminating actin assembly through Rac/Cdc42 GTPase-activating proteins. *Nat. Commun.* **6**, 8623
183. Petiot, A., Faure, J., Stenmark, H., and Gruenberg, J. (2003) PI3P signaling regulates receptor sorting but not transport in the endosomal pathway. *J. Cell Biol.* **162**, 971–9
184. Fratti, R. A., Backer, J. M., Gruenberg, J., Corvera, S., and Deretic, V. (2001) Role of phosphatidylinositol 3-kinase and Rab5 effectors in phagosomal biogenesis and mycobacterial phagosome maturation arrest. *J. Cell Biol.* **154**, 631–644
185. Ross, S. L., Tran, L., Winters, A., Lee, K. J., Plewa, C., Foltz, I., King, C., Miranda, L. P., Allen, J., Beckman, H., Cooke, K. S., Moody, G., Sasu, B. J., Nemeth, E., Ganz, T., Molineux, G., and Arvedson, T. L. (2012) Molecular mechanism of hepcidin-mediated ferroportin internalization requires ferroportin lysines, not tyrosines or JAK-STAT. *Cell Metab.* **15**, 905–917
186. Paradkar, P. N., De Domenico, I., Durchfort, N., Zohn, I., Kaplan, J., and Ward, D. M. (2008) Iron depletion limits intracellular bacterial growth in macrophages. *Blood.* **112**, 866–874
187. Freeman, S. A. A., Goyette, J., Furuya, W., Woods, E. C. C., Bertozzi, C. R. R., Bergmeier, W., Hinz, B., van der Merwe, P. A., Das, R., Grinstein, S., van der Merwe, P. A., Das, R., and Grinstein, S. (2016) Integrins form an expanding diffusional barrier that coordinates phagocytosis. *Cell.* **164**, 128–140
188. Gordon, A. H., Hart, P. D., and Young, M. R. (1980) Ammonia inhibits phagosome-lysosome fusion in macrophages. *Nature.* **286**, 79–80
189. Ip, W. K. E., Sokolovska, A., Charriere, G. M., Boyer, L., DeJardin, S., Cappillino, M. P., Yantosca, L. M., Takahashi, K., Moore, K. J., Lacy-Hulbert, A., and Stuart, L. M. (2010) Phagocytosis and phagosome acidification are required for pathogen processing and MyD88-dependent responses to *Staphylococcus aureus*. *J. Immunol. (Baltimore, Md 1950).* **184**, 7071–7081
190. Alwan, H. A. J., van Zoelen, E. J. J., and van Leeuwen, J. E. M. (2003) Ligand-induced lysosomal epidermal growth factor receptor (EGFR) degradation is preceded by proteasome-dependent EGFR de-ubiquitination. *J. Biol. Chem.* **278**, 35781–90
191. Gruenberg, J., and Stenmark, H. (2004) Opinion: The biogenesis of multivesicular endosomes. *Nat. Rev. Mol. Cell Biol.* **5**, 317–323
192. Lee, W. L., Kim, M.-K., Schreiber, A. D., and Grinstein, S. (2005) Role of ubiquitin and proteasomes in phagosome maturation. *Mol. Biol. Cell.* **16**, 2077–2090
193. Fernandez-Borja, M., Wubbolts, R., Calafat, J., Janssen, H., Divecha, N., Dusseljee, S., and Neefjes, J. (1999) Multivesicular body morphogenesis requires phosphatidyl-inositol 3-kinase activity. *Curr. Biol.* **9**, 55–8
194. Raiborg, C., Bache, K. G., Gillooly, D. J., Madshus, I. H., Stang, E., and Stenmark, H. (2002) Hrs sorts ubiquitinated proteins into clathrin-coated microdomains of early endosomes. *Nat. Cell Biol.* **4**, 394–8
195. Rice, A. E., Mendez, M. J., Hokanson, C. A., Rees, D. C., and Björkman, P. J. (2009) Investigation of the biophysical and cell biological properties of ferroportin,

- a multipass integral membrane protein iron exporter. *J. Mol. Biol.* **386**, 717–32
196. Tse, S. M. L., Furuya, W., Gold, E., Schreiber, A. D., Sandvig, K., Inman, R. D., and Grinstein, S. (2003) Differential role of actin, clathrin, and dynamin in Fc gamma receptor-mediated endocytosis and phagocytosis. *J. Biol. Chem.* **278**, 3331–8
 197. Mero, P., Zhang, C. Y., Huang, Z.-Y., Kim, M.-K., Schreiber, A. D., Grinstein, S., and Booth, J. W. (2006) Phosphorylation-independent ubiquitylation and endocytosis of Fc gammaRIIA. *J. Biol. Chem.* **281**, 33242–33249
 198. Booth, J. W., Kim, M.-K., Jankowski, A., Schreiber, A. D., and Grinstein, S. (2002) Contrasting requirements for ubiquitylation during Fc receptor-mediated endocytosis and phagocytosis. *EMBO J.* **21**, 251–8
 199. Radhakrishna, H., and Donaldson, J. G. (1997) ADP-ribosylation factor 6 regulates a novel plasma membrane recycling pathway. *J. Cell Biol.* **139**, 49–61
 200. Macia, E., Partisani, M., Paleotti, O., Luton, F., and Franco, M. (2012) Arf6 negatively controls the rapid recycling of the β 2 adrenergic receptor. *J. Cell Sci.* **125**, 4026–35
 201. Arjonen, A., Alanko, J., Veltel, S., and Ivaska, J. (2012) Distinct recycling of active and inactive β 1 integrins. *Traffic.* **13**, 610–25
 202. Steinberg, F., Heesom, K. J., Bass, M. D., and Cullen, P. J. (2012) SNX17 protects integrins from degradation by sorting between lysosomal and recycling pathways. *J. Cell Biol.* **197**, 219–30
 203. Buckley, C. M., Gopaldass, N., Bosmani, C., Johnston, S. A., Soldati, T., Insall, R. H., and King, J. S. (2016) WASH drives early recycling from macropinosomes and phagosomes to maintain surface phagocytic receptors. *Proc. Natl. Acad. Sci. U. S. A.* **113**, E5906–E5915
 204. Mitsuuchi, Y., Johnson, S. W., Sonoda, G., Tanno, S., Golemis, E. A., and Testa, J. R. (1999) Identification of a chromosome 3p14.3-21.1 gene, APPL, encoding an adaptor molecule that interacts with the oncoprotein-serine/threonine kinase AKT2. *Oncogene.* **18**, 4891–4898
 205. Mao, X., Kikani, C. K., Riojas, R. A., Langlais, P., Wang, L., Ramos, F. J., Fang, Q., Christ-Roberts, C. Y., Hong, J. Y., Kim, R.-Y., Liu, F., and Dong, L. Q. (2006) APPL1 binds to adiponectin receptors and mediates adiponectin signalling and function. *Nat. Cell Biol.* **8**, 516–523
 206. Wang, Y. B., Wang, J. J., Wang, S. H., Liu, S. S., Cao, J. Y., Li, X. M., Qiu, S., and Luo, J. H. (2012) Adaptor protein APPL1 couples synaptic NMDA receptor with neuronal prosurvival phosphatidylinositol 3-kinase/Akt pathway. *J. Neurosci.* **32**, 11919–11929
 207. Lee, J.-R., Hahn, H.-S., Kim, Y.-H., Nguyen, H.-H., Yang, J.-M., Kang, J.-S., and Hahn, M.-J. (2011) Adaptor protein containing PH domain, PTB domain and leucine zipper (APPL1) regulates the protein level of EGFR by modulating its trafficking. *Biochem. Biophys. Res. Commun.* **415**, 206–11
 208. Miaczynska, M., Christoforidis, S., Giner, A., Shevchenko, A., Uttenweiler-Joseph, S., Habermann, B., Wilm, M., Parton, R. G., and Zerial, M. (2004) APPL proteins link Rab5 to nuclear signal transduction via an endosomal compartment. *Cell.* **116**, 445–456
 209. Bohdanowicz, M., Balkin, D. M., De Camilli, P., and Grinstein, S. (2012)

Recruitment of OCRL and Inpp5B to phagosomes by Rab5 and APPL1 depletes phosphoinositides and attenuates Akt signaling. *Mol. Biol. Cell.* **23**, 176–87

APPENDIX 1

To establish that the Fpn-GFP fusion protein traffics correctly in RAW macrophages, I co-transfected RAW cells with plasmids encoding PM-RFP and Fpn-GFP and fixed the cells without adding a phagocytic target. I observed localization of both markers at the plasma membrane of RAW macrophages (Fig S1A) indicating Fpn trafficking throughout the cell is occurring properly. Next, I determined if Fpn-GFP overexpression perturbed phagocyte function by evaluating the phagocytic capacity of Fpn-GFP expressing cells or untransfected cells. To evaluate this, the average number of internalized beads for untransfected and transfected RAW macrophages after 1 hr incubation with IgG-opsonized beads was compared. Phagocytosed IgG-coated beads were differentiated from those that remained extracellular by staining with a fluorophore-conjugated antibody (not shown). These experiments revealed that RAW macrophages with or without Fpn-GFP expression readily ingested IgG bearing targets, having a nearly identical phagocytic index of ~ 2.5 beads per cell (Fig S1B).

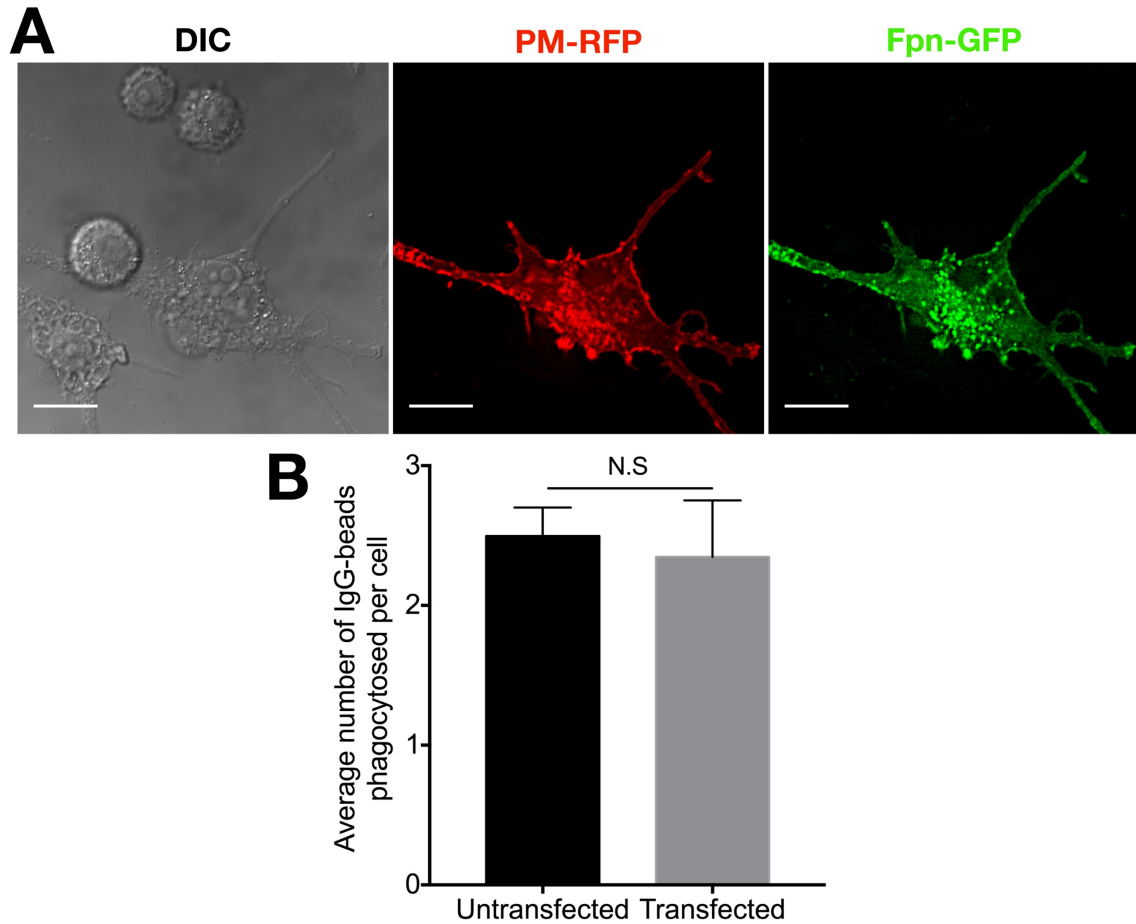


Figure S1. Fpn-GFP localizes to the plasma membrane and does not perturb phagocytosis in RAW264.7 macrophages. (A) RAW cells were co-transfected with PM-RFP (red) and pTF1 (green) and then fixed. Bar equals 20 μ m. (B) Graph depicts the average number of phagocytosed beads per cell in either untransfected RAW cells or RAW cells transfected with pTF1. Data are the mean \pm SD derived from 3 independent experiments. Statistical significance was determined using an unpaired t-test, where n.s is not significant.

CURRICULUM VITAE

Name: Tayler Farrell

Post-secondary Education and Degrees: The University of Western Ontario
London, Ontario, Canada
MSc Candidate 2015-2017: Microbiology and Immunology

The University of Western Ontario
London, Ontario, Canada
BSc (Hons) 2011-2015: Microbiology and Immunology
Dean's Honor List: 2014, 2015

Honours and Awards: Province of Ontario Graduate Scholarship: 2016 - 2017
Value: \$15 000

Western Graduate Research Scholarship: 2015 - 2017
Value: \$9 000

1st Place Poster Presentation Award at Infection and Immunity Research Forum for graduate student < 6 months: November 2015
Value: \$100

Kimberly Clark Award for top 4th year thesis in Microbiology and Immunology: April 2015
Value: \$500

Committee Involvement Infection and Immunity Research Forum Organizing Committee
2014 – 2016

Poster Presentations:

2016

Farrell TJ, Flannagan RS, Heinrichs, DE. June 2016. **Tracking of ferroportin in macrophages demonstrates that it is rapidly removed from the maturing phagosome.** Poster presented at: *66th annual conference of the Canadian Society of Microbiologists*, Toronto, Canada.

Farrell TJ, Flannagan RS, Heinrichs, DE. March 2016. **Tracking of ferroportin in macrophages demonstrates that it is rapidly removed from the maturing phagosome.** Poster presented at: *London Health Research Day 2016*, London, Canada.

2015

Farrell TJ, Flannagan RS, Heinrichs, DE. November 2015. **Tracking of ferroportin in macrophages demonstrates that it is rapidly removed from the maturing phagosome.** Poster presented at: *10th annual Infection and Immunity Research Forum*, London, Canada.